STRONG GROUND MOTION

N.S.F. Seminar-Workshop

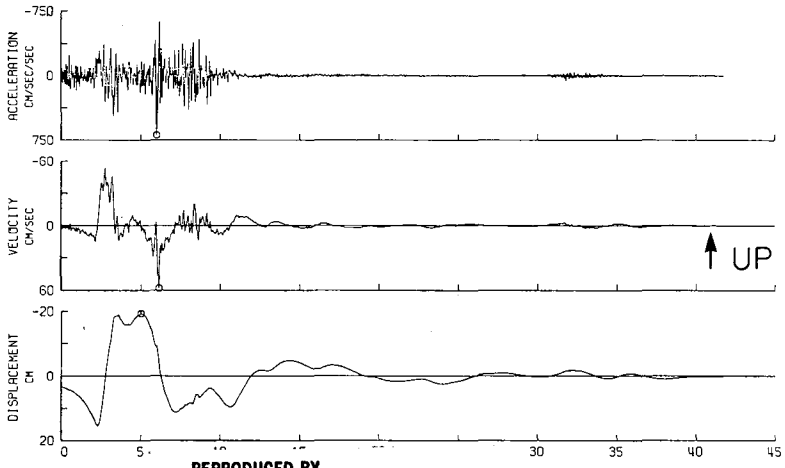

ASRA INFORMATION RESOURCES
NATIONAL SCIENCE FOUNDATION

TABLE OF CONTENTS

Preface..... i

Introduction..... ii

List of Participants..... 1

Program..... 2

Quantitative Prediction of Strong Motion for Potential Earthquake Fault, ... 3

Recent Developments and Applications of Deterministic Earthquake Models: Prediction of Near-And Far-Field Ground Motion..... 6

Application of System Identification Techniques for Local Site Characterization..... 14

Radiated Seismic Energy and the Implications of Energy Flux Measurements for Strong Motion Seismology..... 19

Intensity and Regression..... 25

Modeling of Near-Fault Motions..... 30

A Dynamic Source Model for the San Fernando Earthquake..... 36

Alternative Ground Motion Intensity Measures..... 39

Let's Be Mean..... 41

Measures of High-Frequency Strong Ground Motion..... 46

Synthesis of San Fernando Strong-Motion Records..... 52

SH Propagation in a Layered Half-Space..... 56

Statistics of Pulses on Strong Motion Accelerograms..... 60

An Introduction to Strong-Motion Instruments and Data..... 65

The Application of Synthetic Seismograms to the Study of Strong Ground Motion..... 77

Semi-Empirical Approach to Prediction of Ground Motion Produced by Large Earthquakes..... 80

Deterministic Modeling of Source Mechanisms Utilizing Near- and Far-field Seismic Data: The 1971 San Fernando Earthquake..... 85

Occurrence of Strong Ground Motions..... 89

The Needs of the Nuclear Regulatory Commission in the Field of Strong Motion Seismology..... 92

Some Thoughts on the Definition of the Input Earthquake for the Seismic Analysis of Structures..... 95

Simulations of Earthquake Ground Motions..... 98

Directions of Future Research.....102

PREFACE

The volume represents the Proceedings of a small Seminar - Workshop held at the Inn at Rancho Santa Fe, near San Diego, in February 1978. The meeting was conceived in response to a growing awareness of the mutual interest in research workers in seismology and earthquake engineers in the records of strong ground motion. The Seminar - Wrokshop was partly sponsored by the geophysical and earthquake engineering research programs within the National Science Foundation, and was jointly organized by Donald V. Helmberger of the Seismological Laboratory and Paul C. Jennings of the Earthquake Engineering Research Laboratory, of the California Institute of Technology. The Organizers wish to take this opportunity to acknowledge the helpful assistance of Thomas Hanks, Leonard Johnson and S. C. Liu.

INTRODUCTION

The strong ground motion near the source of a major earthquake determines the forces which endanger buildings and other works of construction, and at the same time is the most detailed clue available concerning the source mechanism of the earthquake. The records obtained of strong ground motion are, therefore, of interest to both seismologists and earthquake engineers, although the two disciplines have tended to look at the records quite differently, and to pursue their examinations separately. In the past few years, however, there has been a growing awareness of the mutual interest in strong ground motion and a number of individuals believed there would be considerable value in convening a small group of seismologists and earthquake engineers who are doing research on strong ground motion for a Seminar - Workshop. It was envisioned that a Seminar - Workshop would be a useful means for scientists and engineers to discuss their mutual interests and problems, and to hear and discuss those areas where their interests and viewpoints are different.

There are many fundamental questions in seismology and earhtquake engineering which focus attention on the nature of strong ground motion. From the seismological viewpoint, the records of strong ground motion provide the best source of high frequency information on the way that energy is released during the rupture process. Additionally, strong motion data has the capability of providing a major means for determining the nature of the source mechanisms in great earthquakes. The extent of the source mechanism, the stress drop and other parameters of the source, and the range of complexity of source mechanisms are all capable of being studied through strong-motion records. From the engineering viewpoint the central problems are the characterization of strong ground motion for the purpose of establishing design criteria and the determination of the nature of the shaking in the near-field of major and great earthquakes. These problems are faced in the design of almost every major facility in the more seismic areas of the country and there is not yet a consensus on how to deal with them. To resolve these important practical problems requires a much increased understanding of strong ground motion. A problem of mutual interest to both seismologists and earthquake engineers is the way the earthquake motion is altered as it propagates away from the source. Seismologists have examined this problem by studies of radiation patterns under idealized conditions and by calculating the effects of regional geology on ground motions of periods of one second and more. Under similar assumptions, earthquake engineers have calculated the effects of surficial soil deposits on strong ground motions of shorter period.

At a few institutions significant interaction between seismologists and earthquake engineers has developed, but there is clearly a benefit to be gained by much more communication between the two disciplines; it was the intent of the Seminar - Workshop to accelerate this communication. It was also hoped that a number of areas of mutual interest and research need could be identified.

This report, which contains extended abstracts of the invited papers, represents the Proceedings and the Seminar - Workshop. The papers and the discussions at the conference were grouped around three major areas.

(1) Characterization and parameterization of strong ground motions.

(2) Simulation and modeling of strong motions: deterministic and statistical.

(3) Source mechanisms and estimation of strong motion for great earthquakes.

The invited papers are followed by a brief discussion of the directions of future research.

D. V. Helmberger

P. C. Jennings

PARTICIPANTS	AFFILIATION
Professor C. Archambeau	C.I.R.E.S.
Mr. J. Beck	Caltech
Mr. J. Boatwright	Columbia University
Professor B. Bolt	U. S., Berkeley
Professor D. Boore	Stanford University
Dr. M. Bouchon	M.I.T.
Professor J. Brune	U.C., San Diego
Professor A. Chopra	U.S., Berkeley
Professor A. Cornell	M.I.T.
Dr. N. Donovan	Dames and Moore
Dr. J. Evernden	U.S.G.S.
Dr. G. Frazier	Del Mar Technical Assoc.
Dr. T. Hanks	U.S.G.S.
Professor G. Hart	U.C., Los Angeles
Dr. T. Heaton	Caltech
Professor D. Helmberger	Caltech
Professor R. Herrmann	Saint Louis University
Professor G. Housner	Caltech
Professor P. Jennings	Caltech
Professor L. Johnson	U.C., Berkeley
Dr. L. Johnson	N.S.F., Geophysics
Professor C. Langston	Pennsylvania State University
Dr. S. C. Liu	N.S.F., RANN
Professor E. Luco	U.S., San Diego
Professor H. Kanamori	Caltech
Dr. R. Matthiesen	U.S.G.S.
Dr. L. Reiter	N.R.C.
Professor J. Roesset	M.I.T.
Professor H. Seed	U.C., Berkeley
Professor S. Smith	U. of Washington
Dr. D. Tocher	Woodward-Clyde Consultants
Dr. R. Wiggins	Del Mar Technical Assoc.

SEMINAR-WORKSHOP ON STRONG GROUND MOTIONS

Program

Sunday, February 12	
6:00 p.m.	Attitude Adjustment Hospitality Suite
Monday, February 13	
9:00-11:00 a.m.	Introductory Session P. Jennings and D. Helmberger NSF Sponsors - L. Johnson and C. Liu
11:30 a.m.-1:30 p.m.	Lunch Break
1:30-5:30 p.m.	Session - Characterization of Strong Ground Motion G. Housner, H. Kanamori, J. Brune, C. Archambeau, T. Hanks, B. Bolt, and R. Matthiesen.
7:00 p.m.	Dinner
8:00-10:00 p.m.	Session - Modeling of Strong Ground Motion San Fernando Earthquake M. Bouchon, C. Langston, and T. Heaton.
Tuesday, February 14	
9:00 a.m.-11:30 a.m.	Session - Modeling of Strong Ground Motion J. Roesset, H. Seed, J. Luco, D. Boore, J. Boatwright, G. Hart, and A. Chopra.
11:30 a.m.-1:30 p.m.	Lunch Break
1:30-5:30 p.m.	Session - Modeling of Strong Ground Motion (Cont'd) L. Johnson, R. Herrmen, R. Wiggins, J. Beck, A. Cornell, N. Donovan, and L. Reiter.
7:00 p.m.	Dinner
8:00 p.m.	Informal Session - Nature of Great Earthquakes
Wednesday, February 15	
9:00-11:30 a.m.	Session - Direction of Future Research
11:30 a.m.-1:30 p.m.	Lunch Break
1:30-3:00 p.m.	Final Session

QUANTITATIVE PREDICTION OF STRONG MOTION FOR A POTENTIAL EARTHQUAKE FAULT

Keiiti Aki, Michel Bouchon
Bernard Chouet, and Shamita Das

Massachusetts Institute of Technology

We describe a new method for calculating strong motion records for a given seismic region on the basis of the laws of physics, using information on the tectonics and physical properties of the earthquake fault.

Our method is based on a new earthquake model, called "barrier model," which is characterized by five source parameters: fault length, width, maximum slip, rupture velocity, and barrier interval. The first three parameters may be constrained from plate tectonics, and the fourth parameter is roughly a constant. The most important parameter controlling the earthquake strong motion is the last parameter, "barrier interval".

The theoretical basis for the "barrier model" comes from a study by *Das and Aki* (1978) of rupture propagation when barriers of high strength material are present on the fault plane. They showed that the following three different interactions between the crack-tip and the barrier can occur, depending on the strength of the barrier relative to tectonic stress.

(1) If the tectonic stress is relatively high, the barriers are broken as the crack-tip passes.

(2) If the tectonic stress is relatively low, the crack-tip proceeds beyond the barrier, leaving behind an unbroken barrier.

(3) If the tectonic stress is intermediate, the barrier is not broken at the initial passage of the crack-tip, but eventually breaks due to subsequent increase in dynamic stress.

A comparison of the slip function, obtained for the case where all the barriers are broken as the crack-tip passes with the case in which one barrier is left unbroken, is shown in Figures 1 and 2. The "barrier model" provides an explanation for the variation of the seismic spectra of small earthquakes with magnitude observed by *Chouet, et al.* (1978). It also explains the major features of the near-field and teleseismic records of the San Fernando earthquake (*Bouchon,* 1978) and the characteristics of surface faulting in many regions (*e.g., Wallace,* 1973; *Tchalenko and Berberian,* 1975).

There are three methods to estimate the "barrier interval" for a given seismic region: (1) surface measurement of slip across fault breaks; (2) model fitting with observed near- and far-field seismograms; and (3) scaling law data for small earthquakes in the region. The "barrier intervals" were estimated for a dozen earthquakes and four seismic regions by the above three methods, as shown in Figure 3. Our preliminary results for California suggest that the "barrier interval" may be determined if the maximum slip is given. The relation

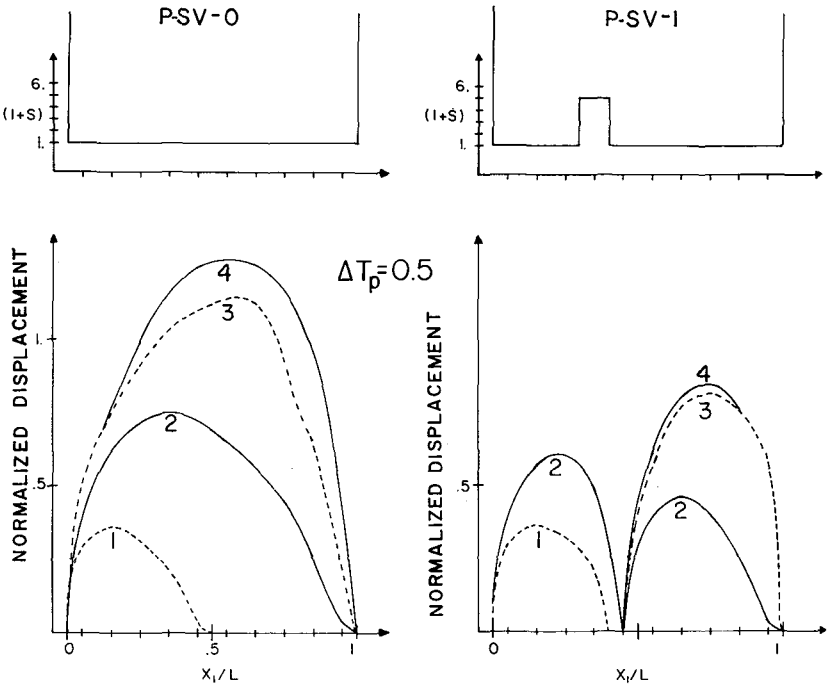

Fig. 1: The Value of (1 + S), a measure of material strength relative to tectonic stress is shown as a function of distance x_1 along the path of rupture propagation on top of the figure. This is the case P-SV-0, in which no barriers exist on the fault plane. At the bottom, snap shots of the parallel component displacement of the crack surface $u_1(x_1,o,t)$ are shown as a function of x_1. u_1 is normalized by the factor $L(\tau_0-\tau_f)/\mu$ and the number attached to each curve indicates time, t, measured in the unit of $0.5L/\alpha$, where L is the length of the fault, α is the compressional wave velocity, μ is the rigidity, τ_o is the initial tectonic stress, and τ_f is the dynamic function of the fault plane.

Fig. 2: Case P-SV-1, in which one barrier exists on the fault palne (see Fig. 1 legend for details). The crack-tip skips the barrier without breaking it.

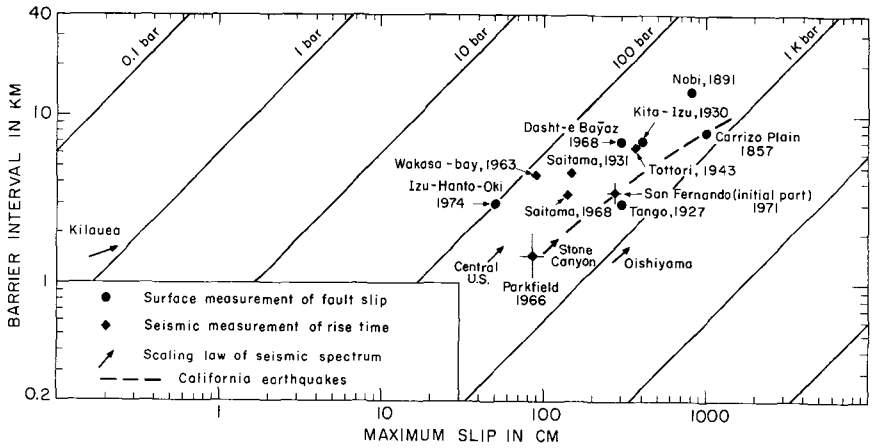

Fig. 3: Relation between the barrier interval and the maximum slip obtained by various methods

between the "barrier interval" and maximum slip varies from one seismic region to another. For example, the interval appears to be unusually long for Kilauea, Hawaii, which may explain why only scattered evidence of strong ground shaking was observed in the epicentral area of the Island of Hawaii earthquake of November 29, 1975.

The stress drop associated with an individual fault segment, estimated from the barrier interval and maximum slip, lies between 100 and 1000 bars (Figure 2). These values are about one order of magnitude greater than those estimated earlier by the use of crack models without barriers. Thus the barrier model can resolve, at least partially, the well-known discrepancy between the stress-drops measured in the laboratory and those estimated for earthquakes.

REFERENCES

Bouchon, M., A dynamic source model for the San Fernando earthquake, Bull. Seis. Soc. Am., submitted 1978.

Chouet, B., K. Aki, and M. Tsujiura, Regional variation of the scaling law of earthquake source spectra, Bull. Seis. Soc. Am., in press, 1978.

Das, S. and K. Aki, Fault plane with barriers: a versatile earthquake model, J. Geophys. Res. submitted 1978.

Tchalenko, J. S. and M. Berberian, Dasht-e Bayaz Fault, Iran: earthquake and earlier related structures in bedrock, Geol. Soc. Am. Bull., 86, 703-709, 1975.

Wallace, R. E., Source fracture patterns along the San Andreas fault, Proc. Conf. Tectonic Processes of the San Andreas Fault System, ed. by R. L. Kovach and A. Nur, Stanford Univ. Press, Geological Sci., Vol. XIII, 248-250, 1973.

RECENT DEVELOPMENTS AND APPLICATIONS OF DETERMINISTIC EARTHQUAKE MODELS: PREDICTION OF NEAR-AND FAR-FIELD GROUND MOTION

Charles B. Archambeau
University of Colorado

There are two objectives of the work to be described. First, to provide an understanding of the near-field ground motion observed from earthquakes in terms of the basic physics of the source; and second, to be able to determine critical physical variables, such as the stress field, prior to an earthquake. From these variables it would be possible to predict not only the probable location and size of future earthquakes, but the expected ground motion as well, and given this ability, to actually be able to make reliable ground motion predictions.

In attempting to realize these objectives it is clearly necessary to accurately account for wave propagation effects in rather great detail. Thus, it is necessary to have a reasonably good, detailed, knowledge of the earth structure, including both anelastic and elastic properties. Based on studies of seismic radiation from nuclear explosions, it is felt that we have sufficiently good analytical and numerical wave propagation methods for these purposes and that our knowledge of earth properties, in at least some regions, is adequate to be able to realistically account for the most important propagational effects.

Of at least equal importance for the achievement of the stated objectives (particularly prediction) is the use of a dynamical theory for the source so that it will be possible to relate the seismic radiation from an earthquake directly to the physical properties of the material and the initial stress state of the medium. Both of these can, in principle be inferred independently before the occurrence of the event. In the work to be described here we have used the dynamical relaxation theory formulation (*e.g., Archambeau,* 1968; *Archambeau and Minster,* 1978), and as preliminary models, the growing spherical inclusion models derived from this theory (*Archambeau,* 1968; *Minster,* 1973). In addition, we have used dynamical boundary conditions on the failure surface enclosing the (narrow) region in which the material transition (failure) occurs and, in particular, the result (*Archambeau and Minster,* 1978) that the rupture velocity is proportional to the stress drop.

In order to determine the detailed physical origins of the radiated field, we have considered the seismic field data from the San Fernando earthquake in rather great detail (*Bache, Barker, and Archambeau,* 1978).

Figure 1 shows a schematic of the symmetry plane for the failure zone, or "fault plane", for the event along with the sense of rupture propagation from the point of nucleation at a depth of 11.4 km. Two relaxation theory models were used to represent these rather complex variable stress drop events; one at the hypocenter that grew bilaterally for approximately 3 km and then extended unilaterally upward until it reached the bend in the failure plane

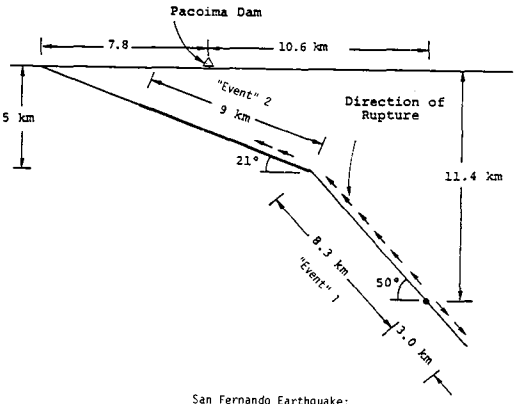

San Fernando Earthquake:
Geometry of the failure zone and location, extent and sense of growth for the two "events" used to model the complete earthquake.

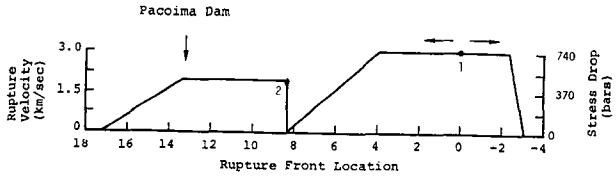

Fig. 1: Rupture velocity and stress drop plotted as functions of distance along the fault from the hypocenter. Event 2 was started from a finite volume for the failure zone while event 1 started from a point.

shown; and a second "event" which forms a continuation of the first beyond the bend beginning with finite failure zone volume and high stress drop and rupture velocity, extending unilaterally toward the surface. The lower graph in the figure shows the variations of stress drop and rupture velocity used, where the rupture velocity was varied directly with the stress drop. This final composite model is the result of many iterations in fitting first the short period far-field, then the long period moment, and finally the near-field strong motion as observed at the Pacoima Dam receiver. This model, therefore, simultaneously fits the long and short period far-field and gives a good first order fit to the Pacoima velocity and displacement records.

Figure 2 shows the fit to the short period (near 1 Hz) seismograms recorded at a number of stations beyond 30° in distance (except for ATL which was near 25°) and at various azimuths. As can be seen, the fit is quite good, certainly for the first 10 seconds, with deviations being most marked at later times at some of the stations. It is likely that some of

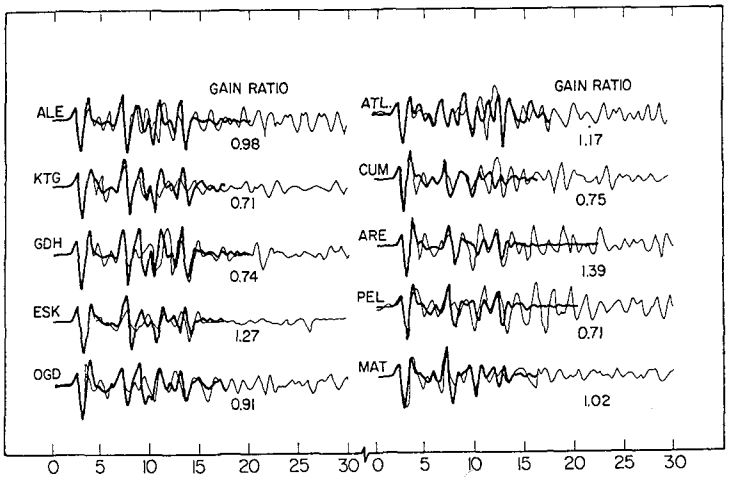

Fig. 2: San Fernando Earthquake: Theoretical (double event) and observed displacement at teleseismic distances.

later "signal" is due to the near surface faulting, which was not included in the model, and that most of it is "signal generated noise"; that is, due to surface waves generated by body wave signal arrivals in the receiver vicinity. This phenomena was not included in the wave propagation calculations and so would not be predicted. It was found that these short period signals could be modeled using only the high stress drop parts of the composite event. On the other hand, the low frequency surface waves and body waves were almost entirely controlled by the low stress drop, low rupture velocity, dimensionally more extensive part of the failure process.

Figure 3 shows the fit of the model predictions to the near-field strong motion data at the Pacoima dam receiver. Clearly the fit to the first 5 to 6 sec. of the displacement record is very good. The deviation at later times, starting near 7 sec. after the start of the signal train, is probably due to the omission from the model of the very-near surface faulting, which involved branching into multiple faults, as well as from omission from the wave propagation calculation of the surface waves generated at the free-surface by the direct waves from the event.

Virtually the same comments apply to the velocity data, in that the fit is fairly good to around 5 sec. for the wave field with frequency below about 2 Hz. However, comparison of the theoretical and observed velocity clearly shows that the model, which fits the short period far-field data very well, does not fit the higher frequency near-field data very well at

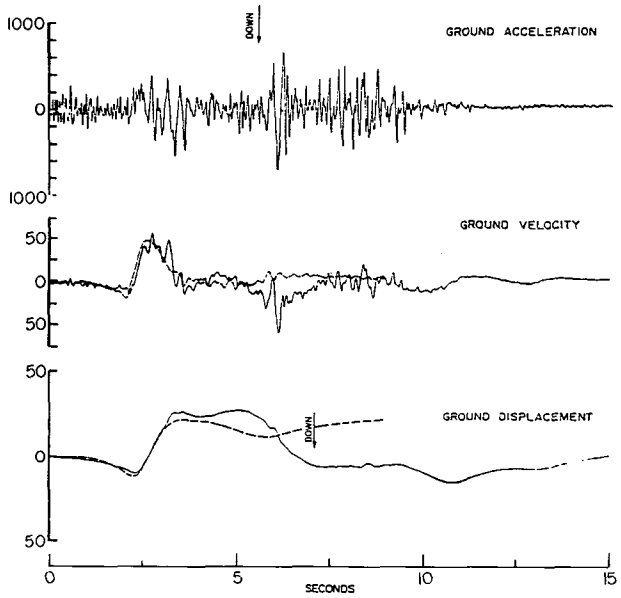

Fig. 3: Comparisons of the observed and predicted (dashed lines) velocity and displacement at the Pacoima Dam site. Final fault model for the San Fernando earthquake.

all. Thus a "far-field model" which fits the seismic data below about 2 to 3 Hz does not provide a very good fit to the high frequency near-field data above 3 Hz. Thus, in both the velocity and acceleration records, the large 3-4 Hz pulse arriving at 3 sec. and 6 sec. from the beginning of the record are not predicted by the "far-field model", nor is the yet higher frequency background signal that is evident on the acceleration records.

Because of the constraints on the model from the (band limited) far-field data and in view of the fit to the near-field low frequency data, the only way to fit the high frequency strong motion data is to include short intervals, of the order of .5 km., of very high stress drops along the failure zone. The stress drops would have to be of the order of several kilobars. In particular, from the data itself, it is evident that one very high stress drop "event" of small dimension (about .1 km.) must have occurred at the hypocenter corresponding to the initiation of failure. Similarly, a second high stress "event" of somewhat larger dimension must have occurred at the fault bend in order to account for the high frequency acceleration and velocity signal arriving at about 3 sec. on the seismograms. The later arriving signals, starting at around 6 sec. and including the maximum acceleration, would

then be explained by a combination of (low stress drop) multiple faulting at the surface and surface wave generation from the earlier large, high frequency signals.

These modifications of the model would alter the stress drop and rupture velocity shown in Figure 1, so that short sections near the points (1.) and (2.) would have very high stress drops, of the order of several kilobars, and correspondingly high rupture rates.

In the context of the dynamical source theory used, these results imply that earthquake failure processes are initiated at stress levels of the order of several kilobars and that growth of the failure zone is accomplished dynamically; that is the failure zone is dynamically driven through zones of relatively low initial stress, with this process occurring because of the high dynamic stress concentrations near the "front" (region of maximum surface curvature) of the failure zone. Further, for stresses of this magnitude, which are of the same order as those observed for failure under laboratory conditions, the dynamic theory requires failure transition energies of the order of 10^7 ergs/gm (see *Archambeau and Minster*, 1978). This transition energy is in fact the change in the internal energy of the material upon failure. The transition energy for melting, for example, ranges from 10^7 to 10^9 ergs/gm in ordinary solids and probably somewhat lower for "weakened" solids. The size of the transition energy implies a nearly complete, although perhaps transient, loss of shear strength and probable melting in the failure zone, or at least melting of some of the rock constituents. Thus, the highly variable stress drop observed for the San Fernando earthquake is interpreted to be a consequence of the inhomogeneity of the initial, ambient, stress field arising, at least in part, from the variability in long term strength of the material to low strain rate loading, as well as from the elastic inhomogeneity of the medium. From this interpretation it would follow that the failure process would initiate at a point at which the highly inhomogeneous stress field reached a critical level of several kilobars. At the time of failure the shear stress drop would be nearly total. The energy changes associated with the ensuing stress relaxation must then be such that the (dynamic) energy density at the edges of the transition zone be large enough to overcome the transition energy barrier--of about 10^7 ergs/gm--in order for the process to continue. Since the energy density near the edges of an inclusion can be much larger than the initial energy density, it is clear that the failure zone may continue to expand into new material even when the origin stress level was not sufficient to initiate failure there.

The conclusion is therefore, that the near-field strong motion data requires very high, localized, stress drops along the failure zone and that it is these spatially limited, high stress drops that result in the very high accelerations in the near-field. It is also concluded that these same high stress points are the locations of failure initiation.

The second objective of predicting near-field accelerations in a deterministic fashion becomes, under the premise that all of the previous conclusions are generally accurate, primarily a question of being able to infer the initial stress field prior to an earthquake. More accurately, prediction of the location, size, and expected radiation field of an earthquake in both the near- and far-fields requires the determination of the "recoverable"

initial stress existing prior to the event. One approach that is currently being applied involves using small earthquakes as events that "sample" the existing stress field. In particular, observations of the radiation fields from small events (foreshocks) may be used to infer the associated stress drops. Since the events are small, it is safe to assume that the accompanying stress changes are small perturbations in the existing background stress, so that these stress drop determinations provide a sampling of the recoverable initial stress.

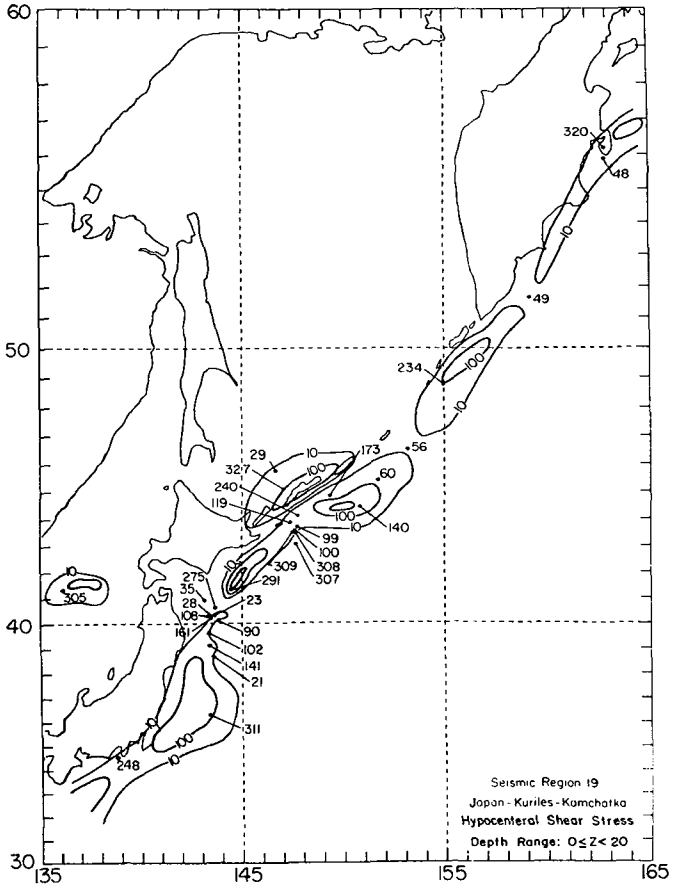

Fig. 4: Shear stress contours for Region 19 in the depth range 0-20 km. Stress changes estimated using m_b and M_s data. Numbers refer to event sequence numbers, the larger values indicating the most recent events. Contours at 10, 100, 1000 bars.

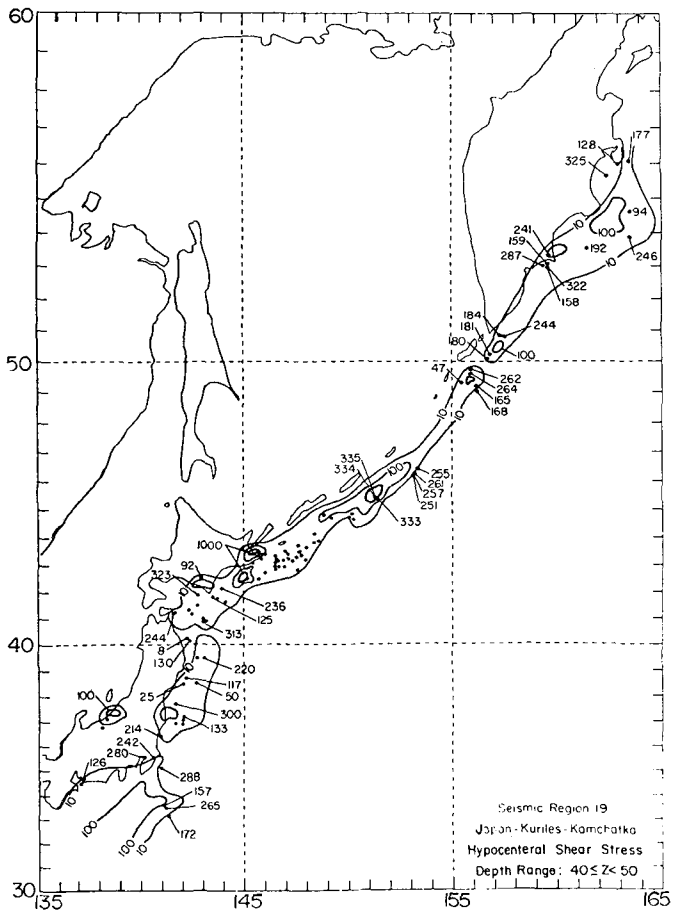

Fig. 5: Shear stress contours for Region 19 in the depth range 40-50 km. Stress changes estimated using m_b and M_s data. Numbers refer to event sequence numbers, the larger values indicating the most recent events. Contours at 10, 100, 1000 bars.

Figures 4 and 5 illustrate recoverable stress maps for different depth ranges obtained using this approach, with event magnitudes as the data from which stresses are estimated for the individual events. When enough small events are available the stress estimate data can be contoured to provide a reasonable first order estimate. Clearly the high stress zones at

or above 1 kilobar, are the sites for future large earthquakes. The larger the dimension of such a very high stress zone, the larger the expected earthquake.

The stresses estimated in this way are average stresses over a volume and fluctuations over small dimensions are not resolved. In view of the necessity of determining the rather small spatial zones of very high stress in order to obtain good near field ground motion predictions, it is clear that a high resolution method must be used to obtain the required stress maps. This means that many very small events must be studied and that high frequency seismic radiation field data must be used so that the stress drop averages obtained are over small volumes. A high frequency method of this type is presently being applied to California micro-earthquake data. Preliminary results from earlier work, using larger earthquakes in Eurasia, suggest that the required resolution can be attained.

REFERENCES

Archambeau, C. B., General theory of Elastodynamic Source Fields, Rev. Geophys, 16, 241-288 1968.

Archambeau, C. B., The theory of Stress Wave Radiation from Explosions in Prestressed Media, Geophys., J.R. astr. Soc., 29, 329-366, 1972,(Appendix, Geophys, J. R. astr. Soc., 31 361-363, 1973)

Archambeau, C. B., and J. B. Minster, Dynamics in Prestressed Media with Moving Phase Boundaries: A Continuum Theory of Failure in Solids, Geophys. J. R. astr. Soc., 52, 65-96, 1978.

Bache, T. C., T. G. Barker and C. B. Archambeau, The San Fernando Earthquake - A Model Consistent with Near-Field and Far-Field Observations at Long and Short Periods. in preparation. From: Final Report, USGS Earthquake Hazards Program, for the period Oct. 1, 1976 to Sept. 30, 1977. Systems, Science and Software, LaJolla, California.

Minster, J. B., Elastodynamics of Failure in a Continuum. Ph.D. Thesis, California Institute of Technology, Pasadena, Calif. 1973.

Minster, J. B. and A. M. Suteau, Far-Field Waveforms from an Arbitarily Expanding, Transparent Spherical Cavity in a Prestressed Medium, Geophys. J. R. Soc., 50, 215-233, 1976.

APPLICATION OF SYSTEM IDENTIFICATION TECHNIQUES FOR LOCAL SITE CHARACTERIZATION

James L. Beck
California Institute of Technology

INTRODUCTION

A question of concern in the earthquake-resistant design process is to what extent and in what manner should the design response spectrum or ground motion time history be modified to account for the influence of local soil and geological properties at the site. To investigate this problem, a model is required which characterizes the dynamics of the local medium in terms of its geometry and material properties. For example, an alluvial-filled valley might be modeled by an elastic region imbedded in an elastic half-space. Alternatively, to greatly reduce the order of a linear model, the local medium might be represented by its dominant modes.

In general, the parameters of such models for a particular site must be determined empirically. If seismic records are available from the site, there is a potential for applying system identification techniques to estimate the parameters and to make some evaluation of the model form.

The general approach formulated in the next section would require at least one ground motion record, the "output", at the surface of the site, together with corresponding records which describe the "input" motion to the model. The number and location of the records necessary to define the input depends on the complexity of the model. For example, for a simple one-dimensional model with vertical wave-propagation, a record from the bottom of a bore hole may be sufficient. In general, some difficulties may arise because a simplified model and its associated input may not define all the input motion to the local region which contributes to the recorded output.

IDENTIFICATION OF DYNAMIC MODELS

It is assumed that the model has been expressed in a discrete form so that its dynamics can be written:

$$\dot{\underline{x}}(t) = \underline{f}(\underline{x}, \underline{u}, t; \underline{a}), \; t \in (T_i, T_f) \quad , \quad \underline{x}(T_i) = \underline{c}$$

where $\underline{x}$ is the state vector of the model; $\underline{f}$ is a function or functional specified by the assumed form for the model; $\underline{u}$ is the input history; $\underline{a}$ is a vector of unknown parameters; and $\underline{c}$ is the initial state, which is generally unknown.

It is assumed that the recorded output, $\underline{y}$, consists of certain components of the state and its rate of change over some time interval, T_i, T_f , so that:

$$\underline{y}(t) = \Gamma_1 \underline{x}(t) + \Gamma_2 \dot{\underline{x}}(t) + \underline{n}(t), \; t \in [T_i \; T_f]$$

where Γ_1 and Γ_2 are rectangular matrices which select the observed components of $\underline{x}$ and $\dot{\underline{x}}$. The term $\underline{n}(t)$ represents the output error between the recorded response and the model response.

The model equation above may be thought of as defining a whole class of models where each member is given by assigning a value to the parameter vector, $\underline{a}$. The aim is to use the recorded input, $\underline{u}$, and recorded output, $\underline{y}$, for the time interval, T_i, T_f, to determine the best model in this class. The best model is defined in the output-error approach to be that model given by the parameters $\hat{\underline{a}}$, which minimize the scalar measure of fit:

$$J(\underline{a}) = \min_{\underline{c}} \left\{ \frac{1}{T_f - T_i} \int_{T_i}^{T_f} \| \underline{n}(t; \underline{a}, \underline{c}) \|^2_{N(t)} \, dt + \| \underline{c} - \hat{\underline{c}}_0 \|^2_C \right\} + \| \underline{a} - \hat{\underline{a}}_0 \|^2_A .$$

Here N(t), C, and A are prescribed weighting matrices, which are symmetric and positive definite, and $\hat{\underline{a}}_0$ and $\hat{\underline{c}}_0$ are prior estimates of the parameters and initial state. In a stochastic framework, N(t), C, and A would be inverse of the covariance matrices of $\underline{n}(t)$, $\hat{\underline{c}}_0$, and $\hat{\underline{a}}_0$. The best model is essentially that model which minimizes a weighted mean-squared output error, but with some constraints governed by the size of the elements of C and A, which prevent too large a departure from the prior estimates $\hat{\underline{c}}_0$ and $\hat{\underline{a}}_0$.

The problem of identifying the best model, therefore, reduces to minimizing $J(\underline{a})$, and this can be tackled by a number of techniques. Two major groups are the filtering methods, which process the data sequentially and lead to sequential estimates of the parameters, and gradient methods, which are iterative methods that use all the data at each iteration (1,2).

Regardless of how this minimization is achieved, an advantage of this formulation is that it allows the assumed model form to be evaluated. Since the best model within the given class is found, if the response agreement is not satisfactory, then it must be the form of the model which is at fault.

APPLICATIONS TO LINEAR MODELS

Two applications, one with simulated data and one with real data, are given to illustrate the above ideas. In both cases, model parameters of a linear model were identified by applying the formulation above. The parameters and initial state were not constrained (i.e., A = C = 0) and the minimization of J was carried out by a successive parameter-minimization algorithm. The technique will be discussed in the author's forthcoming Ph.D. dissertation.

Simulated Data

A ten-degree-of-freedom chain system with uniform mass, stiffness, and damping was subjected to a base excitation given by the first 10 seconds of the N-S component of the 1940 El Centro earthquake record. This system might be used, for example, to model the propagation of vertical SH waves in a flexible elastic layer overlying very stiff material. The acceleration of the top mass, $\ddot{\underline{x}}_{10}(t)$, was computed by numerically solving the relevant equations of

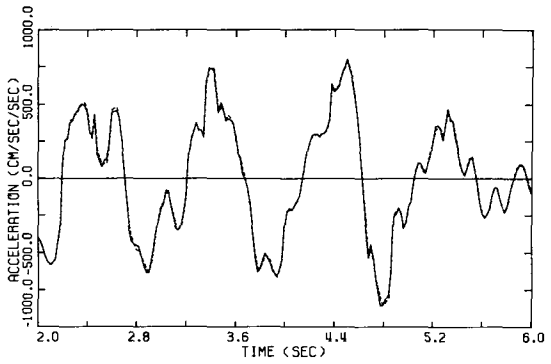

Fig. 1: Acceleration (——) of top mass of uniform chain system, and acceleration (---) of identified four-mode model of system.

motion. The time segments of the excitation and response given by $T_i \approx 2.0$ seconds and $T_f \approx 6.0$ sec. were then used to identify the parameters of a four-mode model of the system. The exact parameters and their estimates from the identification procedure are shown in Table I. Figure 1 illustrates the excellent response matching achieved by the identified model.

Mode	Period (sec)		Damping Factor (%)		Participation Factor	
	Exact	Estimate	Exact	Estimate	Exact	Estimate
1	1.000	1.000	5.00	4.99	1.267	1.265
2	0.336	0.336	5.00	5.00	-0.407	-0.407
3	0.205	0.205	5.00	4.79	0.226	0.214
4	0.150	0.150	5.00	4.33	-0.143	-0.129

Table I. Parameters estimated from the acceleration at the top of a uniform chain system with 10 degrees of freedom.

There is no measurement noise in this simulated-data case. However, there is model error because only a four-mode model was taken, whereas the actual system has ten participating modes. This error has a greater effect on the parameter estimates of the higher modes because of their lower signal-to-noise ratio. The quality of the response match indicates that a four-mode model would be a good representation of the complete system, as far as the earthquake-induced motion of the system is concerned.

Real Data

The same algorithm employed above was applied to strong-motion accelerograph records obtained in the Union Bank Building in Los Angeles during the 1971 San Fernando earthquake. This building is a 42-story steel-frame structure which experienced a peak acceleration of about 20% at mid-height during the earthquake. The longitudinal components of the digitized sub basement and 19th floor velocity records were used to estimate the properties of the first four dominant modes in the longitudinal direction of the building.

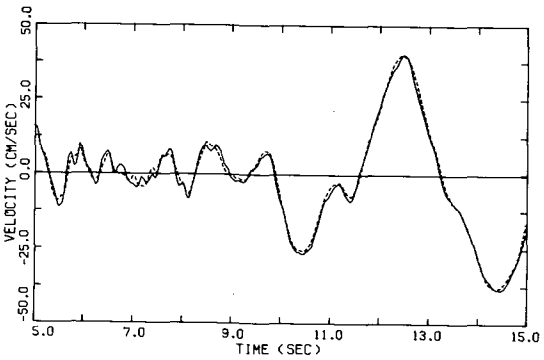

Fig. 2: Velocity (——) at 19th floor of Union Bank Building, and velocity (---) of identified four mode model of building.

Mode	Period (sec)	Damping Factor (%)	Effective Participation Factor
1	4.42	4.1	0.80
2	1.50	6.4	0.57
3	1.12	25	-0.41
4	0.66	8.0	-0.18

Table II. Parameters estimated from the velocity record at the 19th floor of the Union Bank Building.

The values of the estimated parameters using a 10 sec. segment (T_i = 5 sec, T_f = 15 sec) of the records are shown in Table II and Figure 2 shows the corresponding velocity match. All these values, except for those of the "third mode", are consistent with what an engineer might reasonably expect. A close inspection of the Fourier amplitude spectrum of the 19th floor acceleration record indicates that for the third mode the identification procedure has confused two close modes as one mode. These modes appear to be the third longitudinal mode, with a period of about 1.0 sec., and the second torsional mode, with a period of about 1.25 sec. These two modes are not particularly close in the frequency domain, so it is felt that the erroneous results are partly due to neglecting the contribution in the model to the torsional response from the transverse base excitation. This may therefore illustrate the potential difficulties that could arise when some of the input to the real system is ignored in the model.

REFERENCES

Bowles, R. L. and T. A. Straeter, System Identification Computational Considerations, in System Identification of Vibrating Structures, W. D. Pilkey and R. Cohne (eds), ASME, New York, 1972.

Distefano, N. and A. Rath, Modeling and Identification in Nonlinear Structural Dynamics, One Degree of Freedom Models, Report No. EERC 74-15, University of California, Berkeley, California 1974.

RADIATED SEISMIC ENERGY AND THE IMPLICATIONS OF ENERGY FLUX MEASUREMENTS FOR STRONG MOTION SEISMOLOGY

John Boatwright

Lamont-Doherty Geological Observatory
and
Department of Geological Sciences
Columbia University

Recent seismological studies have illustrated that the gross amplitude and frequency content of strong ground motion can be estimated using the elementary source parameters of seismic moment, source radius, and stress drop. In simple source models (*Brune*, 1970), only two of these are independent, and with a constant stress drop assumption, only one is generally taken to be M_o. *Hanks* (1976), using only an estimate of M_o, for the Kern County earthquake, estimated observed measures of strong ground motion for this earthquake, relative to the San Fernando earthquake to ± 50%, at two stations in Los Angeles which recorded them both.

Even so, it is known that earthquake faulting can be considerably more complicated than the two parameter representations of M_o and r are capable of describing. In particular, source propagation (directivity) and the inhomogeneous faulting can have significant influence on the recorded ground motion at certain distances and azimuths. These effects are particularly well quantified in the consideration of the energy flux in a strong motion accelerogram. Analysis of this energy flux, as well as providing an insight on faulting mechanisms, leads naturally to a quantitative estimate of the radiated seismic energy of an earthquake, E_s, a somewhat neglected member of the aforementioned set of elementary source parameters.

The seismic energy flux, at $\underset{\sim}{x}$, in a body wave traveling with velocity $c(\underset{\sim}{x})$, is given by:

$$\dot{\varepsilon}_c(\underset{\sim}{x},t) = \rho(\underset{\sim}{x})\ c\ (\underset{\sim}{x})\ \dot{u}^2\ (\underset{\sim}{x},t),$$

where $\rho(\underset{\sim}{x})$ is the density and $u(x,t)$ is the ground displacement. The time history of the energy flux in a particular body wave arrival may then be represented by a plot of the square of the ground velocity, hereafter referred to as a v^2-plot. This transformation was introduced by Hanks (1974) in a paper discussing the faulting mechanism of the San Fernando earthquake. His v^2-plot of the S16^{o}E component of the Pacoima Dam accelerogram eloquently demonstrateed the heterogeneous character of the earthquake. Despite having a generally faster spectral falloff, the time histories of the energy flux show more detailed pulse shapes than displacement time histories; weaker echoes are suppressed. The dependence of the source strength on the square makes $\dot{\varepsilon}_c(\underset{\sim}{x},t)$ more sensitive to inhomogeneities in the faulting process, as well as to coherence or directivity effects in the radiated body waves. In the absence of coherence effects, such as sharp stopping phases the energy flux directly reflects the energy

release rate of the faulting process, suggesting that measurements of the random components of $\dot{\varepsilon}_c(\underset{\sim}{x},t)$ could be used to constrain statistical models of earthquakes.

A number of velocity time histories and their corresponding v^2-plots, obtained from strong motion accelerograph recordings of a large aftershock of the Oroville earthquake (8/3/76, 0103, M_L = 4.6), which I will refer to as event A, are shown in Figure 1. The nucleation and stopping phases are unusually distinct, particularly in the OAP-SV and 4-SV records. These v^2 calculations, in contrast to displacement calculations, are remarkably uncontaminated by low frequency noise or near-field effects. The velocity time history was obtained from the accelerograms using a parabolic baseline connection which minimized the time-integrated energy flux of the record.

The time-integrated energy flux in a particular body wave is obtained by the integration,

$$\varepsilon_c(\underset{\sim}{x}) = \int \dot{\varepsilon}_c(\underset{\sim}{x},t)\ dt,$$

where the range of the integration should be chosen to isolate the energy flux contained in the arrival. This measurement represents an important constraint for spectral analysis. For any given spectral model, the measurements of low frequency level, corner frequency, and integrated square velocity provide an overdetermined system of three variables and two unknowns. This is particularly useful if the corner frequency cannot be determined with certainty. The quantity

$$n_c = \left(\frac{I_c(x)}{(\bar{u}_c(x),^2} \right)^{1/3}$$

where $I_c(\underset{\sim}{x}) = \dot{u}^2(\underset{\sim}{x},t)\ dt$, and $\bar{u}_c(\underset{\sim}{x})$ is the low frequency level, may be used to obtain an estimate of the source radius from the approximate relation,

$$\eta_\beta = 1.8\ (\frac{v}{r}),$$

where v is the rupture velocity. Estimates of η_β, for event A, are listed in Table 1, along with corner frequency measurements.

The estimation of E_x from measurements of $\varepsilon_c(x)$ is straightforward, although necessarily approximate. The equation relating these quantities, analogous to the relation between moment and low frequency level, is most simply written as

$$E_s = \left(\frac{R(\underset{\sim}{x},\underset{\sim}{\xi})}{Fc(\Theta,\phi)} \right)^2 \frac{\varepsilon_c(\underset{\sim}{x})}{\varepsilon_c(\Theta,\phi)}\ .$$

Here $R(\underset{\sim}{x},\underset{\sim}{\xi})$ is the geometrical spreading factor and $F^c(\Theta,\phi)$ is the radiation pattern correction. The dependence of the radiated seismic energy on the square of the radiation pattern correction presents a major source of uncertainty for single station analysis work. $e_c(\Theta,\phi)$ is

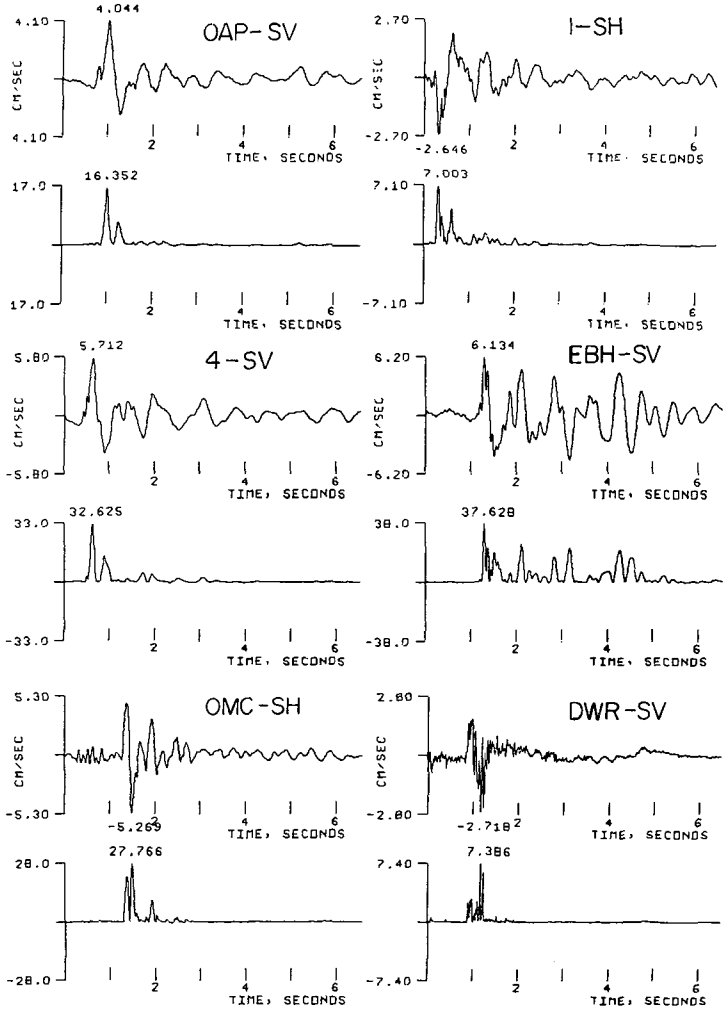
4.044
4.10
OAP-SV
CM/SEC
-4.10
TIME, SECONDS
2.70
I-SH
-2.70
-2.646
16.352
17.0
-17.0
7.003
7.10
-7.10
5.712
5.80
4-SV
-5.80
6.134
6.20
EBH-SV
-6.20
32.625
33.0
-33.0
37.628
38.0
-38.0
5.30
OMC-SH
-5.30
-5.269
2.80
DWR-SV
-2.80
-2.718
27.766
28.0
-28.0
7.386
7.40
-7.40
2
4
6

Fig. 1

Table 1

Station	Comp	$\ddot{u}_{max}$ (cm/sec^2)	M_o (10^{23}ergs)	E_s (10^{18}ergs)	E_s(Vector Sum)	ν_β	η_β
1	SH	80	1.0±.25	4.3±1.2	4.6	1.3	6.2
	SV	140	1.0±.2	4.8±.8		1.2	
3	SH	22	1.1±.3	2.1±.4	1.3	1.2-1.7	4.8
	SV	30	.4±.5	1.0±.3		1.2-2.0	
4	SH	69	.75±.15	6.9±2.4	4.7	1.4-2.3	5.9
	SV	109	1.1±.15	4.4±1.		1.5	
5	SH	105	.9±.15	10.0±2.5	5.5	1.0-2.0	6.5
	SV	162	1.0±.2	3.9±.8		1.5-3.0	
OMC	SH	170	1.1±.4	42.0±14.	21.5	3.0	11.9
	SV	156	.85±.2	1.3±.5		2.2-4.0	
OAP	SH	27	2.1±1.4	19.7±16.	2.3	1.1	5.0
	SV	45	.8±.1	2.1±.6		1.1	
DWR	SH	162	1.5±.2	50.0±42.	6.0	-	-
	SV	208	.4±.8	3.7±1.8		-	
EBH	SH	178	1.15±.2	18.0±3.0	16.8	1.2-2.3	9.2
	SV	168	1.5±.3	16.0±5.0		1.7	

a dimensionless factor which I call the fractional energy flux. It is the ratio of the "normalized"(by $(F^c(\Theta,\phi)/R(\underset{\sim}{x},\underset{\sim}{\xi}))^2$) integrated energy flux in a body wave of wave type c, radiated in a particular direction, to the total radiated seismic energy. In his paper on the spectral theory of seismic sources, *Randall* (1973) calculated $e_\beta = \frac{1}{2\pi}$ for sources without directivity. Observationally and theoretically, $e_c(\Theta,\phi)$ may systematically vary over the focal sphere within a factor of ten for particular geometries of rupture growth and stopping. Resolution of the nature of this variation will require substantial observational work. However, these variations, as they result from systematic variations in $\dot{\varepsilon}_c(x,t)$ over the focal sphere, also have particular importance for source modeling, providing information about directivity and the coherence of rupture healing.

The Oroville aftershock accelerograms (*Hanks*, 1976; *Seekins and Hanks*, 1977) present an excellent test for this data-theoretic approach. Eight large aftershocks (M_L = 4.0-4.9) were recorded by eight or more strong motion instruments, providing substantial coverage of the focal sphere. It is this coverage, as well as the excellent quality of most of the records, which makes the data set a unique test for extensive source modeling work. The event for which I will present a preliminary analysis occurred early in the aftershock sequence, and the coverage is not as complete as it is for some of the later events. The station positions and shear wave polarizations are presented in Figure 2. In Table 1 I have compiled moment and

Fig. 2

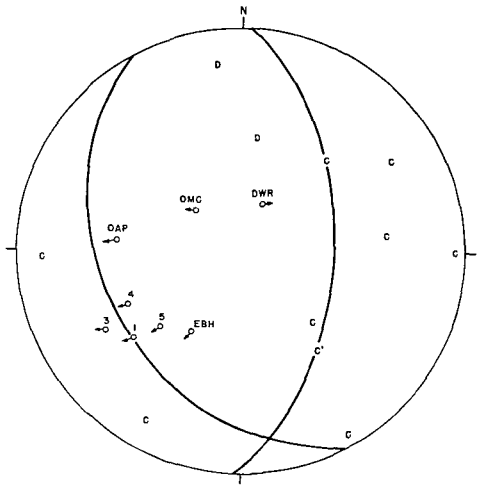

and radiated energy estimates for this event, along with corner frequency measurements and peak accelerations. The radiated energy estimates show a strongly systematic behavior, which is similarly reflected in pulse widths of the v^2 plots of Figure 1. Considering the relative positions of the stations on the focal sphere, it is suggested that these variations are the result of a substantial component of the unilateral rupture updip (to the east) although some modeling work will be necessary to confirm and refine this hypothesis.

REFERENCES

Brune, J. W., Tectonic stress and the spectra of seismic shear waves from earthquakes, J. Geophys. Res., 75 4997-5009, 1970.

Gutenberg, B., and C. F. Richter, Earthquake magnitude, intensity, energy and magnitude, 2, Bull. Seism. Soc. Am., 32, 105-145, 1956.

Hanks, T. C., The faulting mechanism of the San Fernando earthquake, J. Geophys. Res., 79, 1215-1229, 1974.

Hanks, T. C., Observations and estimations of long-period strong ground motion in the Los Angeles Basin, Ear. Eng. and Str. Dyn., 4, 473-488.

Randall, M. J., The spectral theory of seismic sources, Bull. Seism. Soc. Am., 64, 1133-1144, 1973.

Richards, P. G. and J. L. Boatwright, Advanced Research Project Agency semi-annual report, contract #F0098, 1977.

Richter, C. F., Elementary Seismology, W. H. Freeman, San Francisco, Calif., 1958.

Thatcher, W. and T. C. Hanks, Source parameters of southern Californian earthquakes, J. Geophys. Res., 78, 8547-8576, 1973.

Seekins, L. and T. C. Hanks, Strong motion accelerograms of the Oroville aftershocks and peak acceleration data, submitted to Bull. Seism. Soc. Am., 1977.

INTENSITY AND REGRESSION

Bruce A. Bolt

Seismographic Station
University of California
Berkeley, California

Characteristics of seismic intensity remain central to any discussion of strong ground motion. For the great historical earthquakes, the estimation of ground motion parameters depends upon field observations, and even in modern large earthquakes available instrumentation samples only a few points in the meizoseismal zone. Isoseismal lines often define asymmetries and anomalies that challenge explanation by modern seismological theory and seismic wave modeling. This discussion deals with three aspects of intensity: all of which require more careful treatment than previously given.

INTENSITY NEAR FAULTS

A limited number of strong motion accelerograms obtained near a rupturing fault (such as Parkfield in 1966 and Pacoima in 1971) suggest that in such cases the ground near the fault suffers significant pulse-like motions. The pulse amplitude may not be as great as that of the peak acceleration at high frequencies on the same accelerogram, yet because this pulse-like motion has longer dominant periods than the high frequency peak acceleration, it carries much greater mechanical energy capable of doing work on structures. In this regard, there is some evidence from the 1971 San Fernando earthquake that the inelastic displacement of Olive View hospital occurred in the first few seconds of motion, during the early heave of the ground. After this deformation, the building was not greatly affected by the following six to eight seconds of higher frequency acceleration. As a consequence of this behavior, scaling of spectral response using intensities dependent upon high frequency motions may be misleading, with the possiblility of either under- or over-specification of the ground motions. Figure 1 shows an example of a synthetic accelerogram (bottom) constructed from one amplitude spectrum and a different phase spectrum, in order to more closely meet the seismological requirements.

MODELING OF INTENSITY

Isoseismal maps for many large earthquakes are available, which bring to light the relation between source mechanism, geological structure, and local soil conditions. The aim of strong motion seismology is to reproduce, from a small number of seismic parameters, the areal distribution of intensity as mapped, say, in the 1906 San Francisco earthquake. These isoseismal maps often show anomalous regions, sometimes associated with alluvial valleys, but sometimes, surprisingly distributed in terms of expected wave attenuation. A recent example is the asymmetry that occurred in the intensity of the 1977 Romanian earthquake. The inten-

sity pattern is similar to the pattern for the earthquake of November 10, 1940, that also had its focus under the Carpathian Mountains at a depth of about 100 km (see Figure 2). Why is the intensity low in Transylvania to the north of the Carpathians compared with the excessive shaking that occurs to the southeast? Predictions of this intensity from subduction zone models can now be checked against the strong motion record that was obtained in Bucharest in the 1977 earthquake.

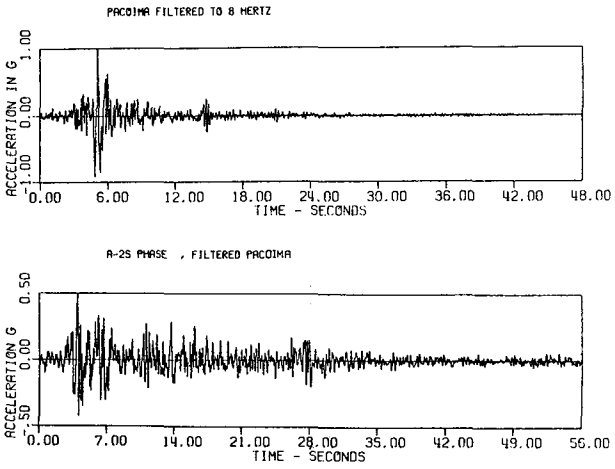

Fig. 1: Example (bottom) of a synthetic accelerogram (horizontal component) produced by combining the amplitude spectrum from one recorded strong motion record (Pacoima) with the phase spectrum of another (called A-2S). At top is the filtered Pacoima record for comparison (computed by Dames and Moore).

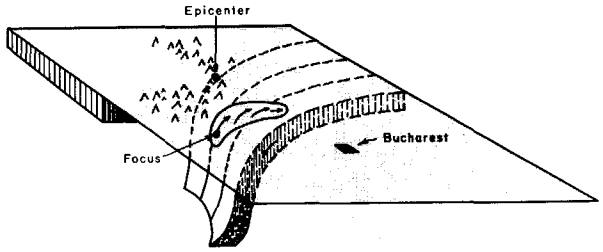

Fig. 2: Diagram of suggested model of the fault rupture (arrows) under the bend of the Carpathian Mountains that produced the Romanian earthquake of 4 March, 1977. This mechanism and geometry gives a general explanation of the character of the strong motion record in Bucharest.

REGRESSION OF INTENSITY AND ACCELERATION

In engineering practice, the peak acceleration assessed for a particular site is often derived from a predicted intensity or earthquake magnitude for the site. Correlations between observed seismic intensity, I, and peak acceleration, A, recorded on instruments in the same area, of the form

$$\text{Log } A = a + b\, I$$

have been derived by a number of authors. In the equation (1) the regression is done assuming the intensity is error-free. In fact, intensity is a random variable with a probability distribution. The correct procedure is to take into account the probability distribution of intensity for each earthquake used in the regression, and use of regression model which allows for the presence of error in both the recorded acceleration (instrumental) and the assessed intensity (field observations).

An example of the frequency distribution for the intensity in the meizoseismal zone of the Truckee earthquake of September 12, 1966, is given in Figure 3, If only the maximum intensity recorded was used, then this earthquake would be given a maximum intensity of X, based on landslides; if the mean intensity was used then VII is appropriate. The former radical bias was not the procedure followed by the USC&GS, and more recently by the USGS, in preparing intensity summaries for United States earthquakes. If the correlations between peak acceleration and intensity are to be used for quantitative purposes as a basis for engineering design, then a more appropriate statistical model must be used in making the regressions between the parameters. It should be added that the same error has arisen in regressing the logarithm of the fault rupture length in earthquakes to their magnitudes. This formula is also used in site evaluations to determine the likely design, earthquake magnitude, and ultimately the peak acceleration for a site. Regressions have been made assuming the independent variable to be error-free, an assumption which is clearly false so far as observed rupture lengths are concerned. (See Figure 4)

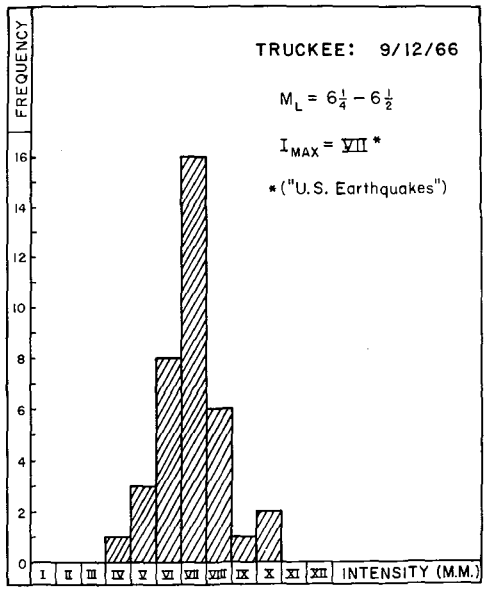

Fig. 3: Histogram of the intensity reports from the meizoseismal zone in the 12 September, 1966 Truckee earthquake. Such histograms show that intensity should be treated as a probability distribution with a central tendency and variance.

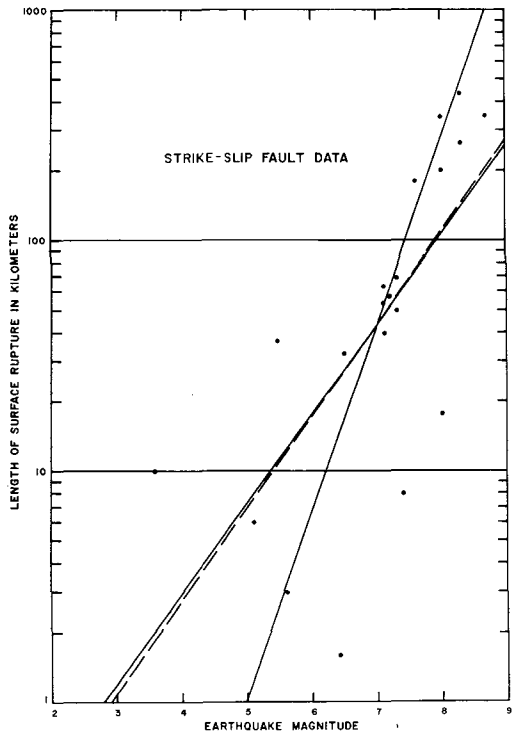

Fig. 4: Regression lines for world-wide data of surface fault rupture and magnitude of the associated earthquake. The order of increasing slope, the lines are (a) regression of log L on M; (b) regression of M on log L assuming L has some error (dashed line); and (c) regression of M on log L treating L as error-free. Curves (a) and (c) are from Mark and Bonilla (1977).

MODELING OF NEAR-FAULT MOTIONS

David M. Boore

Stanford University

Stimulations of strong motion accelerograms using uniform, smoothly propagating dislocations in a homogeneous half-space give records that are much too simple compared to the real thing. To some extent this may be remedied by the inclusion of layering in the system, but we suspect that a significant degree of randomness is characteristic of the real physics of the source process and will have to be incorporated into realistic source models, at least for proper representation of the high-frequency end of the spectrum. Several lines of work are underway:

Rupture Incoherence and Directivity

Computed motions are often sensitive to rupture propagation because of destructive interference of the radiated waves. The interference is particularly strong for low rupture velocities at azimuths away from the direction of fault rupture. These directivity effects are present in all theoretical computations, and if real, clearly have a first order effect on the computed near fault motions. These effects are usually predicted from smooth, coherent ruptures; since we feel that this coherence can be destroyed by irregularities either in fault propagation or in the elastic parameters in the material surrounding the fault (*Brune*, 1976, *Nur*, 1978), the question arises as to the effect of this incoherence on the directivity of the radiated waves from a fault in which rupture velocity and fault slip had statistical distributions along a fault with segments of random length was devised. This analytic expression was checked against Monte Carlo simulations. Figures 1 and 2 show some of the results. We found that the rupture incoherence can increase the high frequency motions, as has been pointed out by a number of other authors (*e.g. Aki*, 1967, 1972; *Haskel*, 1964, 1966; *Das and Aki*, 1977), and that the azimuthal and rupture velocity dependence of directivity still exists, and in fact can be enhanced by the incoherent faulting.

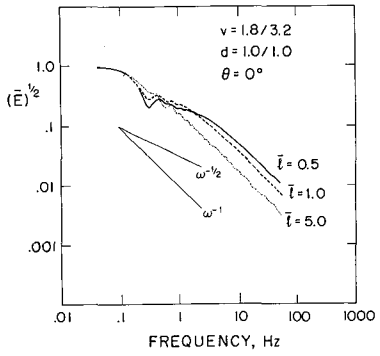

Fig. 1: The influence of coherence length on the mean spectrum for the fault with random variations of rupture velocity between 1.8 and 3.2 km/sec. Note the flattening of the spectrum due to the increase of the corner frequency associated with the coherence length.

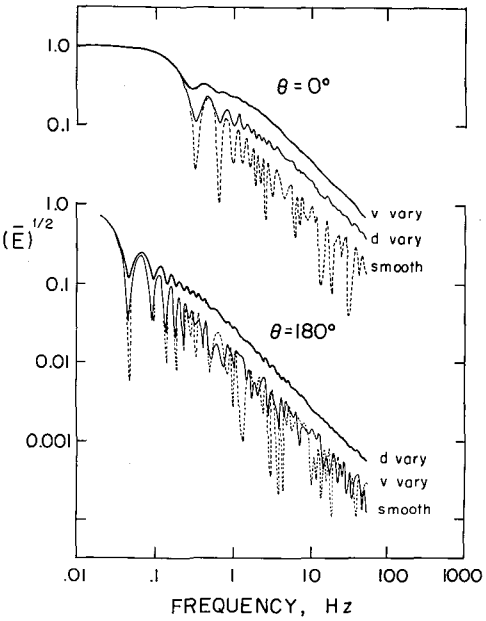

Fig. 2: The mean spectra calculated for forward and back azimuths and three types of faulting: smooth, coherent faulting with 2.5 km/sec rupture velocity and fault flip of 1.0 units; variable rupture velocity ("v vary") with upper and lower limits of 3.2 and 1.8 km/sec, respectively; and variable fault slip ("d vary") between limits of 0.25 and 1.75 units. In the latter two cases the mean of the fault properties was the same as for the smooth rupture. Rupture length was 30 km and coherence length was 1.0 km. A shear velocity of 3.3 km/sec was assumed. Ordinate is in arbitrary units.

A Statistical Simulation Model

A preliminary study of the 1952 Kern County earthquake showed that a multisegment fault would generate realistic looking strong motion records (Figures 3 and 4). In this example the segments were chosen to approximate a smooth rupture, and it was only the small mismatches between segments that produced the complicated motions. This led to the idea of a simulation model based on a complex fault with randomly varying properties (this is an extension and improvement of the model proposed by *Rascon and Cornell,* 1968). The experience gained from the previously discussed study of rupture incoherence has been incorporated into a first generation form of such a simulation model. An example of a simulation of the accelerogram recording at Temblor during the 1966 Parkfield, California earthquake (see Figure 5 for the geometry) is shown in Figure 6. In this Figure we compare the data (top) to a smooth rupture and to ruptures with mean velocities of 2.5 and 2.9 km/sec which start at the epicenter and propagate southeast to a point somewhat beyond Gold Hill. The bottom trace shows the motion from a unidirectional rupture starting near Gold Hill and propagating along the fault away from Temblor. As expected directivity effect is pronounced. Adding a small amount of rupture to the southeast would have increased the amplitude (but not the duration) of this record.

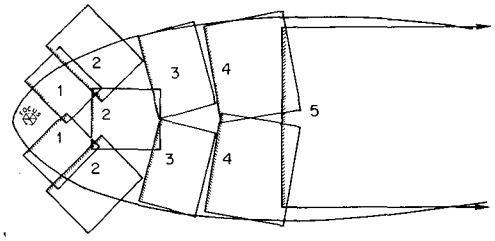

Fig. 3: Schematic of 1952 Kern County earthquake rupture surface. Rupture started at the left side.

Fig. 4: Comparison of waveforms for the Pasadena recording of the Kern County earthquake.

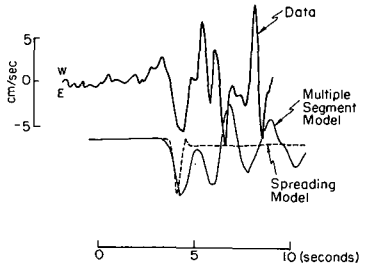

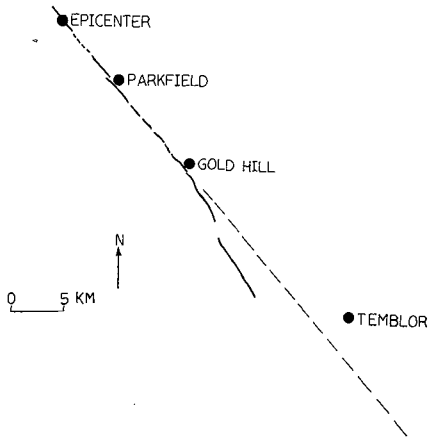

Fig. 5: Geometry of Parkfield simulation.

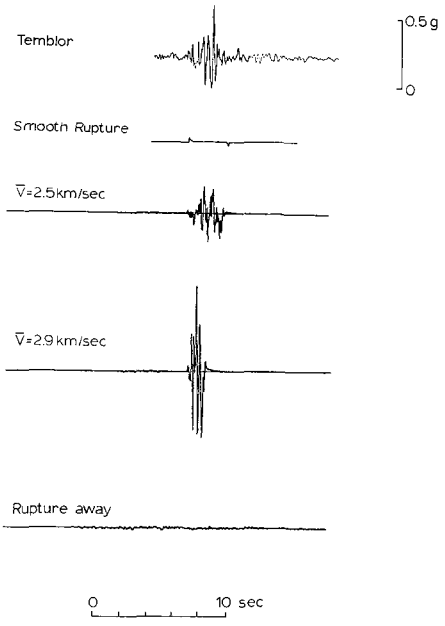

Fig. 6: Simulation of Temblor recording with a complex fault.

Surface Waves in Strong Motion

Moving away from the generation of high frequencies by complex faults, at lower frequencies geologic structure can have an important influence on the motions; and for ground displacements in particular, the dominant motions may be best described as surface waves. We are investigating the simulation of these types of motions using straightforward modal superposition. There are many advantages to this technique: an almost arbitrarily complicated layered structure can be used; P and SV type motion is as easy to generate as Sh motion and all multiple bounces are included (this is not true of the often used Cagniard-de Hoop technique); simulations for any source type (including propagating sources of finite width) and distance are very inexpensive to simulate once the dispersion parameters are calculated -- and these can be quickly evaluated using existing programs. Figure 7 shows an encouraging comparison between data (top), the complete solution for a multilayered half space (middle, taken from *Heaton and Helmberger*, 1978), and our surface wave solution (bottom).

The modeling of existing data is about the only means we have of estimating the physical properties of the faulting process (such as effective stress and rupture velocity). If the multitude of studies of the Parkfield records is at all representative, there may be more uncertainties in the derived fault parameters of various earthquakes than is usually acknowledged. The problem is that these parameters are then accepted as being valid and used in the

derivation of subsequent parameters--after awhile one wonders what to believe. For example in a recent attempt to survey the literature for determinations of rupture velocity (which seems to have a first order effect on ground motions), I came across a table in which rupture velocities of 2.3 km/sec and 3.5 km/sec were the most common entries; on closer examination almost all of these values were taken from the papers of one researcher. To illustrate the nonuniqueness, I repeated one of the waveform simulations using a velocity of 3.2 km/sec and a larger rise time to make up for the sharpening of the pulses due to the faster propagation velocity. The result in Figure 8 speaks for itself. (Interestingly, the tabulator pointed to this particular earthquake as one for which the rupture velocity was well constrained.)

The point I'm raising is that if we are to use parameters from past earthquakes to guide our simulation of ground motions, a critical reevaluation of these derived parameters may be necessary.

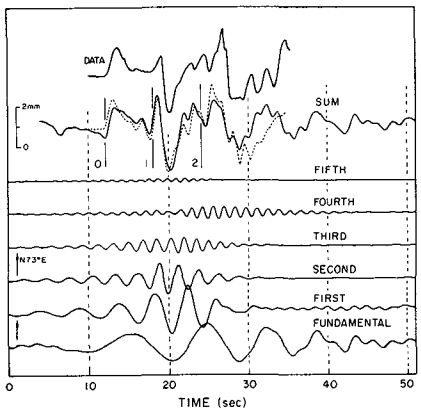

Fig. 7: Data and synthetics for the transverse component of the IVC recording of the Brawley earthquake, 11-4-76. The range is about 33 km and the source depth is about 7 km. Data and Cagniard synthetic are from Heaton and Helmberger (1978). (The dashed line is the Cagniard solution.)

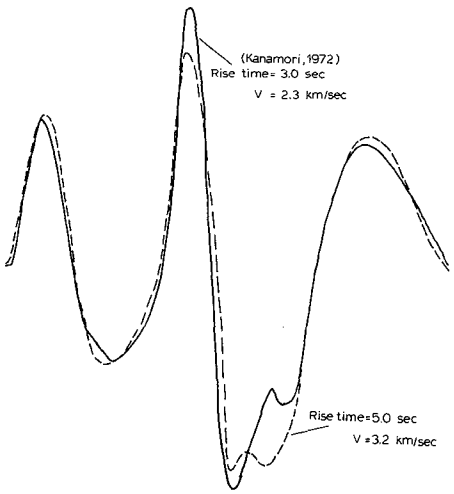

Fig. 8:

REFERENCES

Aki, K., Scaling law of earthquake source time function, Geophys, J. R. astr. Soc., 31, 3-25, 1972.

Brune, J. N. The Physics of earthquake strong motion, ch. 5 in Seismic Risk and Engineering and Engineering Decisions (C. Lomnitz & E. Rosenblueth, ed.), Elsevier Scientific Publ. Co., Amsterdam, 140-177, 1976.

Das, S. and K. Aki, Fault plane with barriers: a versatile earthquake model, J. Geophys. Res. 82, 5658-5670, 1977.

Haskell, N. A., Total energy and energy spectral density of elastic wave radiation from propagating faults, Bull. Seism. Soc. Am. 54, 1811-1841, 1976

Haskell, N. A., Total energy and energy spectral density of elastic wave radiation from propagating faults, Part II. A statistical source model, Bull. Seism. Soc. Am. 56, 125-140.

Heaton, T. H. and D. V. Helmberger, Predictablility of strong ground motion in the Imperial Valley: modeling the M 4.9, Nov. 4, 1976 Brawley earthquake, Bull. Seism. Soc. Am., 1978, (in press).

Nur. A., Nonuniform friction as a physical basis for earthquake mechanics: a review, subm. to Pure and Applied Geophysics., 1978.

Rascon, O. A. and C. A. Cornell, Strong motion earthquake simulation, MIT School of Engr. Res. R-68-15, 155 pp., 1968.

A DYNAMIC SOURCE MODEL FOR THE SAN FERNANDO EARTHQUAKE

Michel Bouchon

Massachusetts Institute of Technology

We present a study of the rupture mechanism of the San Fernando earthquake. In the near-field we model the earthquake as a two-dimensional propagating rupture in a half-space. We synthesize the strong ground motions and accelerations at the Pacoima Dam site using the discrete horizontal wave number method of *Bouchon and Aki* (1977). We take for the slip-time-history on the fault plane analytical expressions which approximate the slip functions of dynamic crack models obtained by *Das and Aki* (1977, 1978). These models allow for the presence of barriers or obstacles on the fault plane. Such barriers are made of high-strength material and may remain unbroken after the passage of the rupture front. Their presence results in a strong enhancement of the high-frequency radiation. This can be seen in Figure 1 where the velocity waveforms synthesized at the Pacoima Dam site and radiated by the upper part of the fault for a uniform dislocation model (A) and for a crack with barriers model (B) are compared. Two major features of the Pacoima Dam accelerograms--the strong pulse associated with the beginning of the rupture, and the high-acceleration phase which arrives in the middle of the records and lasts almost until the end of the disturbance--which are not compatible with a smooth rupture process are well explained by a crack with barriers model. An example of synthesis of the ground acceleration at the Pacoima Dam site is shown in Fig. 2.

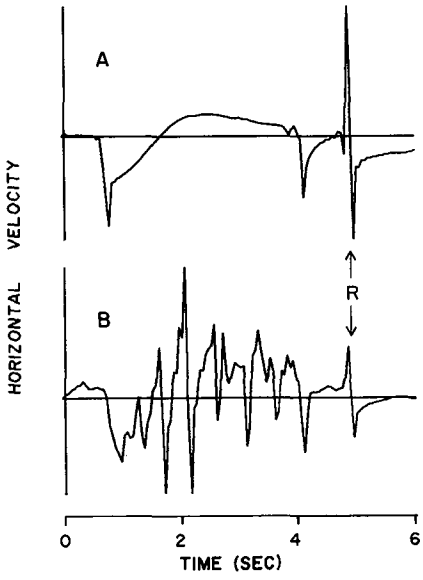

Fig. 1: R indicates the Rayleigh wave radiated by the upper tip of the fault.

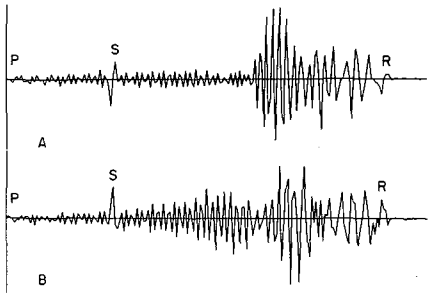

Fig. 2: Horizontal (A) and vertical (B) accelerograms synthesized at the Pacoima Dam site for a crack with barriers model. The beginning of the accelerograms corresponds to the arrival of the P-wave from the hypocenter. The shear wave radiated from the hypocenter (S) and the Rayleigh wave generated at the upper tip of the fault (R) are identified. The cut-off frequency is 10 Hz and the total length of the signal is 9.6 sec.

The P wave short period teleseismic records are characterized by a high amplitude-short duration first pulse indicative of a massive and localized initial rupture (*Hanks*, 1974). We model this initial rupture event as an expanding circular shear crack stopping suddenly. A comparison of the calculated pulse with the data yields a value of the source radius of the initial rupture event of about 1.5 km and a stress-drop on the order of 500 bars. This indicates a high level of tectonic stress in the region. A rectangular fault with randomly distributed barriers is used to model the rest of the rupture process at teleseismic distance. Such a model produces ripples on the seismograms, quite similar to the ones present on the records.

A study of the earthquake series following the main shock shows that the aftershocks which take place in the region where major slip occurred during the earthquake may represent the release of some of the barriers.

Our interpretation of the rupture process is the following: the earthquake starts with a massive and localized initial rupture indicative of a high tectonic stress. The limited areal extent of this initial rupture shows the presence of barriers of very high strength in the hypocentral region. Skipping these barriers, or partially breaking them, the rupture progresses mostly upwards, encountering a large number of barriers of small areal extent which offer a strong resistance to the propagation of the rupture.

REFERENCES

Bouchon, M. and K. Aki, Discrete wave-number representation of seismic source wave fields, Bull. Seis. Soc. Am., 67, 259-277, 1977.

Das, S. and K. Aki, A numerical study of two-dimensional spontaneous rupture propagation, Geophys. J. Roy. astro. Soc., 50, 643-669, 1977.

Das, S. and K. Aki, Fault plane with barriers: a versatile earthquake model, J. Geophys. Res. 1978, (in press).

Hanks, T. C., The faulting mechanism of the San Fernando earthquake, J. Geophys. Res., 79 1215-1229, 1974.

ALTERNATIVE GROUND MOTION INTENSITY MEASURES

C. Allin Cornell

Massachusetts Institute of Technology

There are reasons to consider alternatives to peak acceleration (or velocity or M. M. Intensity) as scalar measures of ground motion intensity. In particular an ordinate of the Fourier amplitude spectrum of acceleration (at, say 1 hz) suggests itself, see Figure 1. We study this (and other) alternatives, first, as they function as predictors of structural response, and, second, as they can be predicted from typical event variables (magnitude, M, and hypocentral distances, R). Together the "errors" (statistical dispersions) in these two predictions determine how well structural response can be predicted from M and R (via a scalar intensity measure, see Figure 2).

We compare, too, peak acceleration alone as it can be predicted directly from distance and M. M. epicentral intensity, I_0, versus its prediction from R and I_0 via magnitude or via M. M. site intensity. There are biases in the latter two paths, paths which may be necessary in regions where strong motion data is effectively non-existant, see Figure 3.

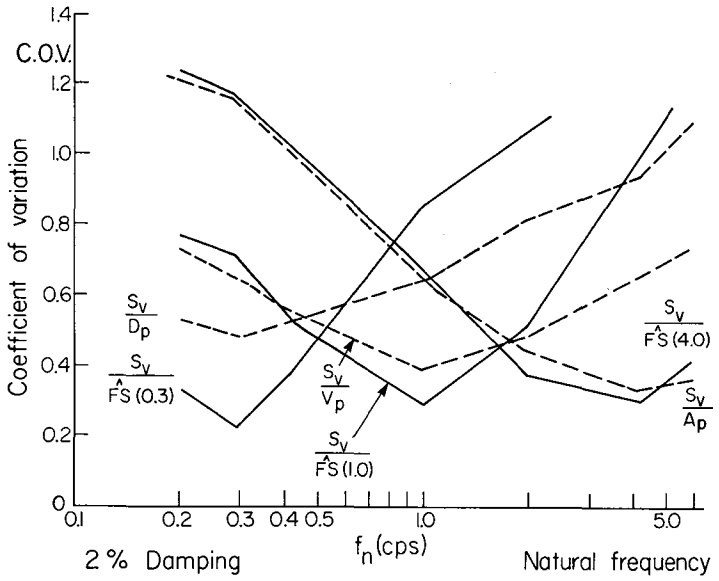

Fig. 1

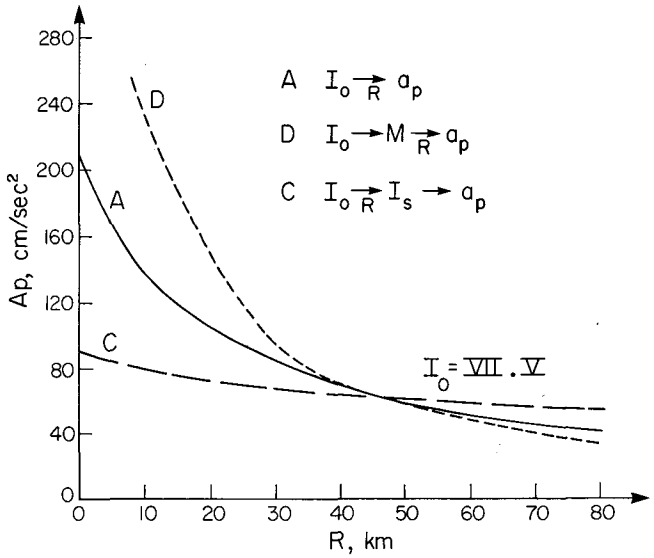
280
240
200
160
120
80
40
0
Ap, cm/sec²
0
10
20
30
40
50
60
70
80
R, km
A
D
C
A $I_o \xrightarrow{R} a_p$
D $I_o \rightarrow M \xrightarrow{R} a_p$
C $I_o \xrightarrow{R} I_s \rightarrow a_p$
I_o = VII . V

Fig. 2

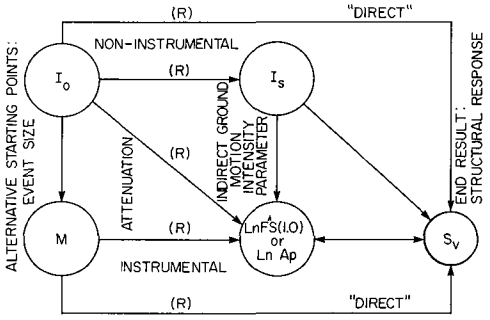
(R)
"DIRECT"
NON-INSTRUMENTAL
I_o
(R)
I_s
ALTERNATIVE STARTING POINTS: EVENT SIZE
ATTENUATION
(R)
INDIRECT GROUND MOTION INTENSITY PARAMETER
END RESULT: STRUCTURAL RESPONSE
M
(R)
LnFS(I.O) or Ln Ap
S_v
INSTRUMENTAL
(R)
"DIRECT"

Fig. 3

LET'S BE MEAN

Neville C. Donovan

Dames & Moore

These notes and attachments are intended to provoke discussion, but must at the same time be accepted as my own personal viewpoints. These views probably disagree with those of other workshop members, and if so, useful discussion should ensue.

The first point I would like to make is a plea that we make an effort to move away from a fixation on the search for a maximum of peak quantities associated with earthquakes. Instead of the premise that the peak instrumental relationship is a function of the number of instruments deployed, we should recognize the simple statistical expectation that as the sample gets larger, the expectation that a larger value will be obtained increases. Fortunately, while we chase around looking for the extreme, we obtain a mean value that becomes increasingly reliable and we gain more information about the scatter of the data values about the reliable mean. From the statistical point of view the Pacoima Dam record is not of special interest. If we carefully keep track of mean values together with the statistics related to the distribution about the mean, we are proceeding in a fashion analogous to following the center of the road while at all times knowing how wide the road is. Other processes lead to either an unknown position on this road, which might even approximate a random walk, or an attempt to follow the indeterminate yet precipitous edge.

How we handle the data we have is also important. There are many ways that established routine processes can bias data. Bollinger showed this first, but I would like to demonstrate it also with an example where all the hard work was done by others.

The event which occurred in Washington State on December 14, 1872, has attracted a lot of interest through its importance to nuclear power plant siting. A study supported by a group of utilities in the Pacific Northwest supplied intensity values for specific sites and intensity isoseismals. The usual pattern of an isoseismal map is familiar, so I would like instead to show the data in terms of Figure 1, where individual values are plotted as small circles and the equivalent isoseismal radius value is plotted as a triangle (isoseismals could be well approximated by a circle). The biasing produced by drawing isoseismals is readily apparent by comparing the circles and the triangles positions, but let us do some least squares fitting. Figure 2 shows the separate best fits to individual points and equivalent radii and demonstrates that the bias in the equivalent radii method is about 3/4 of an intensity--hardly a mean!

The tables attached show the difference between the mean and the value one standard deviation larger computed by several different investigators for three parts of the strong motion problem. These are: (1) peak acceleration, (2) velocity to acceleration ratios, and (3) special amplification values. If one is to follow, as is often suggested, the practice of a value one standard deviation larger than the mean value, the end spectral values could be

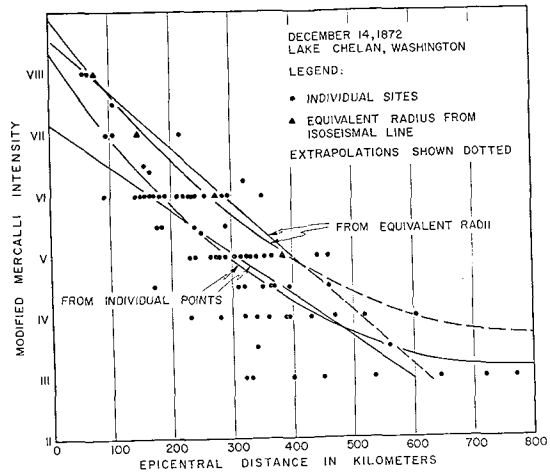

Fig. 1: Individual MM Intensity versus distance data points derived from historic descriptions for December 14, 1872 Washington State earthquake and Intensity versus distance values obtained from isoseismal map.

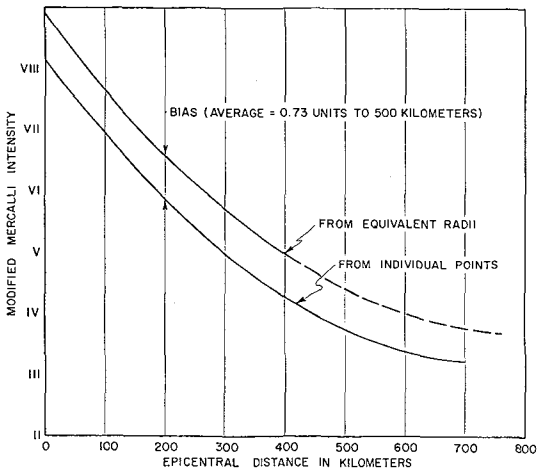

Fig. 2: Lines based on least squares fit showing the bias to attenuation estimate when the quivalent isoseismal radii are sued instead of individual MM Intensity values obtained from felt report distance.

more than four times larger than the most probable value. Surely we have a need for knowing both where the middle of the road is and how wide it is.

Although much research has been done, the scientific and engineering fraternities are still unable to predict ground motions with any precision. The recorded motions from the Humboldt Bay Nuclear plant and site response studies have been used as the basis for a Type A (before the fact) prediction claim by using the free-field values to compute motion levels inside the structure. The full prediction, however, would also require information regarding the free-field motions which the present state of our knowledge is unable to do. Figure 2 shows what happens with attempts to predict the peak acceleration. All fall grossly short of the observed motion and show that Type A claim is only valid when a substantial part of the problem answers are known in advance. The choice of peak acceleration for this example was made for convenience. The actual choice of parameter for comparison is relatively minor. I do recommend that some other parameter than peak acceleration be more widely used and discussed. Maybe we should directly measure something else!

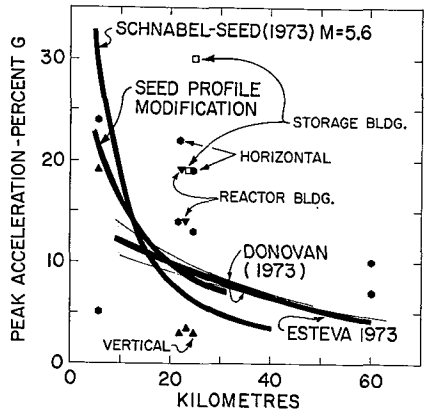

Fig. 3: Instrumental peak acceleration values recorded during the June 7, 1975 Ferndale Earthquake (Magnitude approximately 5.5 with a 20 kilometer focal depth).

TABLE 1

Estimates of Uncertainty

	Author		Standard Deviation Lognormal	Factor
a) accerleration				
	Esteva	1970	1.02	2.8
	Esteva & Villaverde	1973	0.64	1.9
	Donovan*	1973	0.48	1.6
	Donovan	1973	0.71	2.0
	Donovan & Bornstein**	1975	0.3 →0.5	1.3→1.7
	Seed et al***	1976	0.34→0.51	1.4→1.7
	McGuire	1974	0.51	1.7
b) velocity				
	Esteva	1970	0.84	2.3
	Esteva & Villaverde	1975	0.74	2.1
	McGuire	1974	0.63	1.9
c) displacement				
	McGuire	1974	0.76	2.1

* San Fernando data only
** Site specific relationship
***Seed,et.al data are sorted by site characteristics and consider only one magnitude level

TABLE 2

Ground Motion Parameter Ratios

	v/a	v/a	v/a	v/a	Standard Deviation Factor	
	Newmark-Hall	Seed et al	Mohraz		Mohraz	
Profile Type	cm/sec/g	cm/sec/g	cm/sec/g			
			L*	S*	L	S
Rock	61(24)**	66(26)	61(24)	69(27)	1.58	1.63
Stiff Soil	--	114(45)	--	--	--	--
Deep Sand	--	140(55)	76(30)	91(36)	1.53	1.61
Alluvium	122(48)	--	122(48)	145(57)	1.44	1.49

* Mohraz considered horizontal data in two sets. L comprises the set containing the largest horizontal component from each site and the S set contains the lower value.
**Numbers in parentheses are in units of inches/sec/g.

TABLE 3

Spectral Uncertainty

Damping Level	Averaged Across Spectra Blume-Newmark	Mohraz	Seed et. al
Average	1.42	1.41	--
	1.37	1.36	1.4
	1.30	1.31	--

REFERENCES

Donovan, N. C., A statistical evaluation of strong motion data, including the February 9, 1971 San Fernando earthquake, proceedings of the Fifth World Conference on Earthquake Engineering Rome, Itly, 1252-1261, June 1973.

Donovan, N. C. and A. E. Bornstein, A review of seismic risk applications, second International Conference on Applications and Statistics and Probability in Soil and Structural Engineering, Aachen, Vol. III, 1975

Esteva, L., Seismic Risk and Seismic Design Decisions, Seismic Design for Nuclear Power Plants, The MIT Press (edited by Robert J. Hansen), Cambridge, Massachusetts, 142-182. 1970.

Esteva, L. and R. Villaverde, Seismic Risk, Design Spectra and Structural Reliability, unpublished report University of Mexico, 1973.

Hall, W. J., B. Mohraz and N. M. Newmark, Statistical Studies of Vertical and Horizontal earthquake spectra, prepared for the United States Nuclear Regulatory Commission, NUREG-003, January, 1976.

McGuire, R. K., Seismic Structural Response Risk Analysis, Incorporating Peak Response Regressions on Earthquake Magnitude and Distance, School of Engineering, Massachusetts Institute of Technology, Cambridge, R74-51 Structures Publication 99, 1974.

Mohraz, B., A Study of Earthquake Response Spectra for Different Geological Conditions, Bull. Seism. Soc. Amer., 66, No. 3, 915-935, June 1976.

Newmark, N. M. and W. J. Hall, Seismic Design Criteria for Nuclear Reactor Facilities, Proceedings of the Fourth World Conference on Earthquake Engineering, Santiago, Chile, Vol. II, B4 37-50, 1969.

Seed, H. B., C. Ugas and J. Lysmer, Site Dependent Spectra for Earthquake-Resistant Design, Bull. Seism. Soc. Amer., 66, No. 1, 221-255, February 1976.

Seed, H. B., R. Murarka, J. Lysmer, and I. M. Idriss, Relationships between Maximum Acceleration, Maximum Velocity, Distance from Source and Local Site Conditions for Moderately Strong Earthquakes, Bull. Seism. Soc. Amer., 66, No. 4, 1323-1342. 1976.

MEASURES OF HIGH-FREQUENCY STRONG GROUND MOTION

Thomas C. Hanks

United States Geological Survey

Since the first strong motion accelerograms were written more than forty years ago, peak acceleration has been the most commonly used, single index of strong ground motion. It has, however, been known for some time that peak acceleration need not be--and too often cannot be--a uniformly valid measure of strong ground motion over the entire frequency band and amplitude range of engineering interest. The very character of the peak acceleration datum as a short period, time-domain amplitude measurement is the principal reason for two important limitations on its value as a measure of strong ground motion. First, for $M \gtrsim 5$ earthquakes at close distances, taken here as a rough threshold of potentially damaging ground motion, the period of this phase is much shorter than the faulting duration. Thus the peak acceleration simply cannot measure gross source properties of potentially damaging and destructive earthquakes, even if such data may, in a large enough set of observations, indicate limiting conditions on the failure process in very localized regions of the fault surface. Secondly, this same characteristic of the peak acceleration datum makes precise corrections for wave propagation effects, including anelastic attenuation and elastic scattering, impossible except under very unusual conditions. Both of these problems, but especially the second, are in turn responsible for the notoriously large scatter in peak acceleration data, even through very small variations of magnitude, distance, and site conditions. And it is this last problem that limits the utility of peak acceleration even as a measure of high-frequency strong ground motion.

These difficulties in interpreting, manipulating, and using peak acceleration data are widely acknowledged, I believe, by investigators of strong ground motion, whether they be engineers or seismologists. My own interest in these problems has arisen in connection with recently acquired peak acceleration data at small magnitudes ($M \lesssim 5$) and close distances ($R \gtrsim 10$ km) (*Hanks and Johnson,* 1976; *Seekins and Hanks,* 1978), and in those studies we have discussed these issues extensively. But none of that discussion is particularly informative about the really important issue: if peak acceleration is not a reliable measure of high-frequency strong ground motion, as is generally agreed to be the case, then what is? In this correspondence, I will suggest such a measure based on simple earthquake source models that indeed seems better than peak accelerations and perhaps might be.

Simple *displacement* spectral models of the far-field shear radiation of earthquakes are specified by the long period level, Ω_o, proportional to seismic moment, M_o, the corner frequency, f_o, proportional to reciprocal source dimension, f, (or reciprocal faulting duration, T_d) and high-frequency* ($f > f_o$) spectral decay of the form $(f/f_o)^{-\gamma}$. A variety of observations, including m_b-M_s data, peak accelerations as a function of M at $R \gtrsim 10$ km, the wealth of observations for the San Fernando earthquake (at frequencies as high as 100 x f_o), as well

as single station spectral determinations for a large number of earthquakes, suggests that the $\gamma = 2$ model is the one generally, although certainly not always applicable, at least in the frequency band of engineering interest (*e.g., Aki*, 1967; *Berrill*, 1975; *Tucker and Brune*, 1977; *Hanks*, 1978).

Figure 1 presents the *acceleration* spectral amplitudes for the $\gamma = 2$ case for far-field shear waves for two earthquakes at the same R in the presence of anelastic attenuation. The two earthquakes have been assigned the same stress drop $\Delta\sigma$; in the Ω_o-f_o notation of *Hanks and Thatcher* (1972). This means

$$\Omega_o^{(1)} \; (f_o^{(1)})^3 = \Omega_o^{(2)} (f_o^{(2)})^3 \quad , \tag{1}$$

since

$$\Delta\sigma = \frac{7}{16} M_o/r^3 = 106_{\rho} R\Omega_o f_o^3 \tag{2}$$

where ρ density. The anelastic attenuation of spectral amplitudes is taken to be of the form $\exp(-\pi fR/Q\beta)$, where f is frequency, β is shear-wave velocity, and Q is specific attenuation. In Figure 1, f_{max} is the frequency where the argument of the exponent is 1. Then one, non unique interpretation of Figure 1 is that the corresponding acceleration time histories are band limited ($f_o \leq f \leq f_{max}$), finite duration ($0 \leq t\text{-}R/\beta \leq T_d$), white noise. The whiteness arises from the constant acceleration spectral amplitudes equal to $\Omega_o f_o^2$ in the band $fo \leq f \leq f_{max}$, but the randomness has simply been assumed.

The idea that ground acceleration time histories can be taken as band limited, finite duration, white noise is a reasonable one in view of the generally chaotic nature of strong motion accelerograms in finite time windows and frequency bands for $M \gtrsim$ earthquakes. Indeed, this same notion has been the basis for considerable work in the analysis of existing accelerograms and in the computation of synthetic accelerograms for more than 30 years in the engineering community (*e.g. Housner*, 1947; *Hudson*, 1956; *Bycroft*, 1960; *Housner and Jennings*, 1964; *Jennings et al.*, 1968). It is a pleasure to welcome these investigators to the community of $\gamma = 2$ proponents, at this however belated date.

In any event, the root-mean-square acceleration a_{rms} of the acceleration time history corresponding to the acceleration spectra in Figure 1 can be obtained through an application of Parseval's Theorem:

---

*In source mechanism parlance the expression "high-frequency" means frequencies greater than the corner frequency, but in the sense of structural engineering, this expression generally means vibrations at frequencies of several Hz or greater. In this study we are using "high-frequency" in the former sense. Since corner frequencies of $M \gtrsim$ earthquakes are less than 1-2 Hz, the engineering sense of this expression is contained within the seismological one used here.

$$|a(t)|^2 dt \equiv \frac{1}{2\pi} \int |\tilde{a}(w)|^2 dw \qquad (3)$$

where $a(t)$ is the acceleration time history, $\tilde{a}(\omega)$ is its Fourier amplitude spectrum, and ω is circular frequency. Ignoring contributions outside the ranges $0 \leq t-R/\beta \leq f \leq f_{max}$, we write (3) as

$$|a(t)|^2 dt = \frac{2}{2\pi} \int_{}^{2\pi f_{max}} |\tilde{a}(w)|^2 dw \qquad (4)$$

The rms acceleration is

$$a_{rms} \equiv \frac{1}{Td} \int |a(t)|^2 dt \quad ^{1/2} \qquad (5)$$

Equations (2) and (3), together with

$$\tilde{a}(w) = \Omega o (f_o 2\pi)^2, \; f_o \leq f \leq f_{max} \qquad (6)$$

and

$$f_o = \frac{1}{Td}$$

result in

$$a_{rms} = \sqrt{2} \; (2\pi)^2 \; \Omega o f_o^3 \sqrt{\frac{f_{max}}{f_o}} \qquad (7)$$

or, using (2)

$$a_{rms} = \frac{\sqrt{2} \; (2\pi)^2}{102} \frac{\Delta\alpha}{\rho R} \quad \frac{f_{max}}{f_o} \qquad (8)$$

Table 1 compares a_{rms} values estimated from (8) with those "observed" for the San Fernando earthquake at Pacoima Dam and the Kern County earthquake at Taft. The "observed" values are those given in Volume I of the series "Strong Motion Earthquake Accelerograms," corrected by (record length/Td)$^{1/2}$ to estimate the (larger) a_{rms} value that occurs in the time interval of the S-wave arrival through the S-wave arrival plus T_d. Because the accelerations are non zero outside of this interval, the "observed" values are overestimates of the actual a_{rms} values, $0 \leq t-R/\beta \leq T_d$. In any case, however, the agreement between the estimated and "observed" values is remarkable, by conventional seismological standards, in estimating high-frequency amplitudes, being approximately 50% in the case of the San Fernando

earthquake and 20% in the case of the Kern County earthquake.

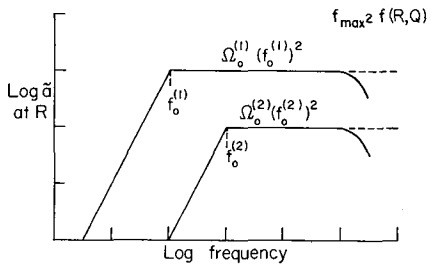

Fig. 1: Far-field shear wave acceleration spectra at R for two constant stress drop earthquakes.

Table 1

Comparisons of Estimated and Observed a_{rms} Values

San Fernando Earthquake		Kern County Earthquake
Feb. 9, 1971; M_L = 6.4		July 21, 1952; M = 7.7
10^{26} dyne-cm	M_o	2 x 10^{27} dyne-cm
10 km	r	25 km
50 bars	$\Delta\sigma$	60 bars
0.1 Hz	f_o	(0.04 Hz)
at Pacoima Dam		at Taft, California
~ 10 km	R	~ 40 km
25 Hz	f_{max}	7 Hz
	a_{rms}	
140 cm/sec^2	estimated	36 cm/sec^2
220, 240 cm/sec^2	"observed"	42, 42 cm/sec^2

There is nothing new in the suggestion that a_{rms} is an important index of strong ground motion nor in the recognition that a_{rms} is related to the spectral amplitudes of ground motion, specifically through (3) and (5). The point I wish to emphasize is that a_{rms} can also be related to physical parameters of the gross faulting process and source-station path, through (8). Thus, empirical correlations of a_{rms} with other physical variables can be set within a theoretical or predictive framework, which in turn can be used to estimate a_{rms}

(and therefore spectral amplitudes of high-frequency strong ground motion) in the absence of any ground motion observations, provided one can realistically choose $\Delta\sigma$, f_o, R and Q for the source-station combination of interest.

Even so, the only really important issue is how well this measure of high-frequency strong ground motion works, in both an observational and theoretical sense. Observationally, the issue is whether or not a_{rms} determinations obtained from ground motion time histories show less scatter than peak accelerations for the same set of other variables, specifically M, R, and site conditions. Theoretically, the issue is whether or not we can predict, to the desired level of accuracy the observations in terms of $\Delta\sigma$, f_o, R, and Q with appropriate allowance for site conditions. The remarkably good agreement between the estimated and "observed" a_{rms} values for the two important accelerograms discussed earlier is encouraging in the latter connection, but considerably more effort must be devoted to both issues. The Oroville aftershock accelerograms appear to be a particularly valuable resource for these investigations. Finally, since (7) and (8) are built on the far-field representation of the $\gamma = 2$ model, it can be expected to fail close enough to a large enough shock, unless we specifically account for the near-field effects that can (but need not) affect periods of a second or so and longer. Otherwise we would be clever enough to break big earthquakes into small enough analytical chunks.

REFERENCES

Aki, K., Scaling law of seismic spectrum, J. Geophys. Res., 72, 1212-1231, 1967.

Berrill, J. B., A study of high-frequency strong ground motion from the San Fernando earthquake, Ph.D. Thesis, California Institute of Technology, Pasadena, 1975.

Bycroft, G. N., White noise representation of earthquakes, J. Engg. Mech. Div. ASCE, 86, 1-16, 1960.

Hanks, T.C., b-values and $\omega^{-\gamma}$ seismic source models, Proceedings of Conference III - Fault Mechanics and its Relation ot Earthquake Prediction, Office of Earthquake Studies, U.S. Geological Survey, Menlo Park, Calfiornia, 1978

Hanks, T. C., and D. A. Johnson, Geophysical assessment of peak accelerations, Bull Seismol. Soc. Amer., 66, 959-968, 1976.

Hanks, T. C., and W. R. Thatcher, A graphical representation of seismic source parameters, J. Geophys. Res., 77, 4393-4405, 1972.

Housner, G. W., Characteristics of strong-motion earthquakes, Bull. Seism. Soc. Amer., 37, 19-31, 1947.

Housner, G. W., and P. C. Jennings, Generation of artificial earthquakes, J. Engg. Mech. Div. ASCE, 90, 113-150, 1964.

Hudson, D. W., Response spectrum techniques in engineering seismology, World Conference on Earthquake Engineering, Berkeley, California, 1956.

Jennings, P. C., G. W. Housner, and N. C. Tsai, Simulated earthquake motions, Earthquake Engineering Research Lab., California Institute of Technology, Pasadena, California, 1968

Seekins, L. C., and T. C. Hanks, Strong motion accelerograms of the Oroville aftershocks and peak acceleration data, Bull. Seism. Soc. Amer., in press, 1978.

Tucker, B. E., and J. N. Brune, Source mechanism and m_b-M_s analysis of aftershocks of the San Fernando earthquake, Geophsy. J. R. Astr. Soc., 49, 371-426, 1977.

SYNTHESIS OF SAN FERNANDO STRONG-MOTION RECORDS

Thomas H. Heaton and Donald V. Helmberger

Seismological Laboratory
California Institute of Technology

Three-dimensional models of a finite fault located in a half-space are constructed to study the ground motions from the 9 February 1971 earthquake as observed at JPL, Palmdale, and Lake Hughes (Array Station #4). The Cagniard-De Hoop Technique is used to compute the ground motions due to infinitesimal point sources which are evenly distributed (0.5 km spacing) on the fault plane. The responses are summed with time lags determined by the assumed hypocentral solution and rupture velocity. Nonuniform fault displacement is modeled by varying the weights of individual point sources. By investigating the motion due to small sections of the fault it is possible to understand how various wave types interfere to produce the motion due to the total fault. Recent modeling of teleseismic body waves by Langston has indicated that the fault changes dip from 50^{o} to 30^{o} at a depth of approximately 5 km. This feature has been incorporated into our models. The assumed fault geometry and station locations are shown in Figure 1. In Figure 2, we display assumed fault displacements for a preliminary model which is used to explain the motions at JPL, PLM, and LKH. The overall moment for this model is 1.5×10^{26} ergs. The hypocenter is assumed to lie in the region of maximum displacement and a rupture velocity of 1.8 km/sec (as suggested by Langston) is also assumed. Although stations LKH and JPL are situated at roughly equal epicentral distances, there appears to be a dramatic difference in the character and amplitudes of ground motion seen for these stations. This can be seen in Figures 3 and 4. In these figures, the synthetic ground motions for the fault model described above are compared with the integrated accelerograms for these stations. Because the integrated accelerograms have been filtered with an 8 sec. Ormsby filter, the synthetics are displayed both with and without the inclusion of this filter. Although it appears that the particular fault model used for Figures 3 and 4 is not, in detail, correct, it does well at explaining the differences in character and amplitude of ground motions as seen between JPL and LKH. An examination of Figure 5 helps one to appreciate the complex interplay between source and wave propagational effects. In this figure the fault is subdivided into 5 strips each of which has a width of 4 km. Also shown are synthetic motions (JPL, North) for a single point source located in the middle of each subfault. Although these point sources produce easily interpreted specific arrivals, it is clear that the JPL record results from complex and not easily interpreted interaction of both source and propagation effects. These synthetics also demonstrate the dramatic effect of the free-surface. Rayleigh wave and sP head wave contributions are of great importance.

The effects of even more complicated earth structure in these records is yet to be studied, but detailed synthesis of records for simpler aftershocks should add some insight to this problem.

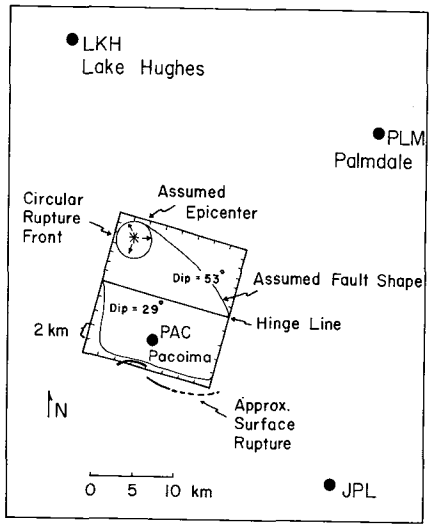

Fig. 1: Assumed geometry for the San Fernando fault and receivers. Model consists of a three dimensional finite fault in a half-space. A Green's function technique is used to integrate the exact solution for a point dislocation over the rectangular grid shown. A circular rupture front propagates from an assumed hypocenter and displacement magnitudes are prescribed on the fault surface.

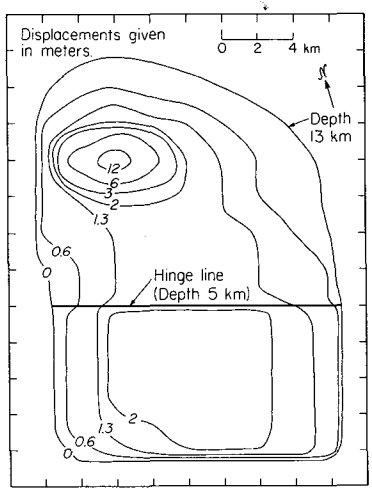

Fig. 2: Contour map of assumed fault displacements for the preliminary San Fernando model displayed in Figures 3, 4, and 5.

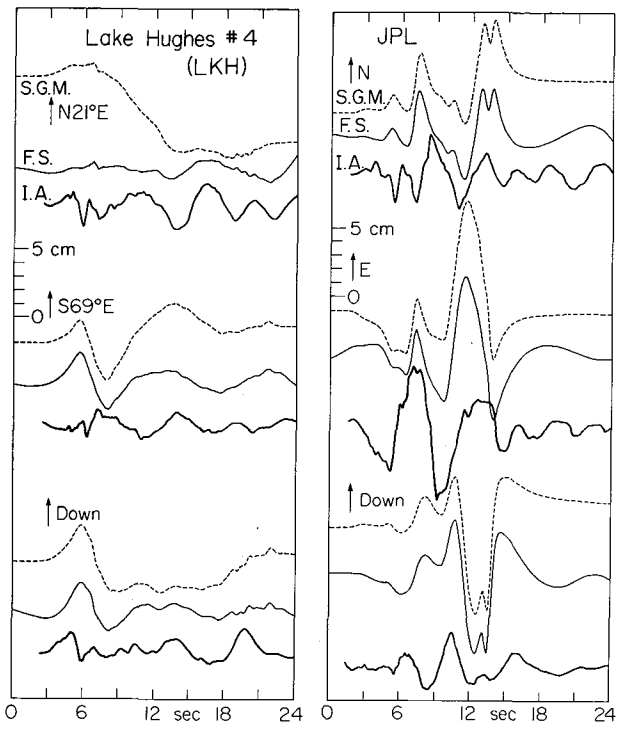

Fig. 3 and 4: Preliminary model of JPL and LKH displacement records. Massive faulting at depth of 13 km and a rupture velocity of 1.8 km/sec. are assumed. The top trace is the synthetic ground motion; the middle trace is the synthetic ground motion filtered with an 8 sec Ormsby filter; and the bottom trace is the observed displacement which has also been filtered at 8 sec. Notice the contrast between the records at JPL and LKH which lie at approximately equal epicentral ranges.

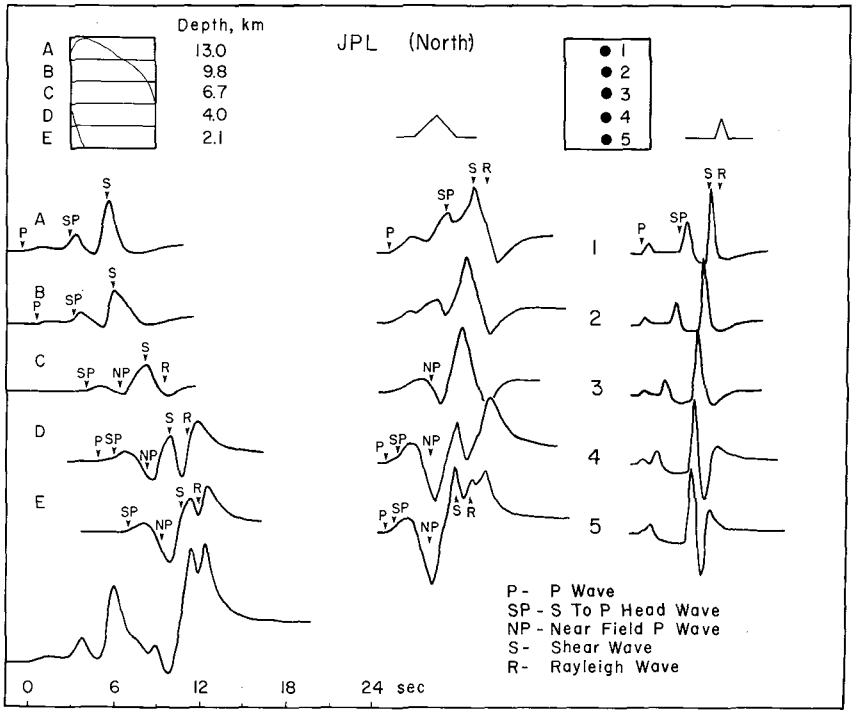

Fig. 5: Decomposition of the N component of synthetic ground motion for JPL. The finite fault is broken into 5 strips whose individual contributions are shown on the left. Responses of point sources which lie in the middle of these strips have been convolved with both 3 sec. and 0.8 sec. triangular far-field time functions and are displayed in the middle and on the right, respectively. By studying the point source responses, contributions of individual phases can be recognized in the synthetic for the finite fault. Notice the complex interplay of source and wave propagational effects.

SH PROPAGATION IN A LAYERED HALF-SPACE

Robert B. Herrmann

Saint Louis University

The formal solution of seismic wave generation and propagation by a point dislocation earthquake source in a layered medium has been presented by *Haskell* (1964) and *Hudson* (1969). The method assumes that the earth can be modeled by a stack of plane homogeneous layers. The solution is obtained by performing a double integration over frequency and wavenumber of form:

$$u(r,\phi,z,t) = \int_{-\infty}^{\infty}\int_{-\infty}^{\infty} u(k,\phi,z,\omega) J_n(kr) e^{-i\omega t} dk\, d\omega .$$

For a non attenuating medium, the wavenumber integration is complicated by the presence of branch points and poles along the real k-axis. The problem can be modified through the use of contour integration in the complex k-plane to avoid numerical problems due to these singularities. The problem is further complicated in this case because the contour integration requires the use of the Hankel function $H_n^{(2)}(kr)$ and the modified Bessel function $K_n(\tau r)$. *Herrmann* (1977) presented a numerical solution to the SH contribution to tangential displacements when contour integration is used. The numerical contour integration techniques used provide valid results at distances as close as one-third the source depth and have been extended to distances of 500 km and to frequencies as high as 10 Hz.

The purpose of this study is to generate realistic transverse wave time histories for some central United States earth models in order to obtain an insight on the nature of ground motion time histories, maximum ground motion parameters, and response spectra.

As an example of the computations, some results are given here for the simple case of a single layer overlying a half-space. In the layer β_1 = 3.55 km/sec and ρ_1 = 2.8 gm/cm^3, while in the half-space β_2 = 4.67 km/sec and ρ_2 = 3.3 gm/cm^3. A point vertical strike-slip source with a seismic moment of 1.0 E 20 dyne-cm is placed at a depth of 10 km in a 40 km thick crust. The time derivative of the dislocation time history and its corresponding spectrum are given in Figure 1. Figures 2 and 3 show the computed displacement, velocity, and acceleration time histories at distances of 50 km and 400 km, respectively. A low pass filter at 1.0 Hz was used. The displacement and acceleration time histories were computed from the velocity time history, assuming the velocity to be composed of linear segments. Figures 4 and 5 show the corresponding response spectra for 0, 2, 5, and 10% damping. Of interest in a preliminary interpretation is the observation that while the maximum ground displacement, velocity, and acceleration vary as r^{-1} over this distance range, the response spectra varies as $r^{-0.6}$ at certain periods. The response spectra also become more complex with distance, just as the time histories become more complex due to the layering effects. *Herrmann* (1977) showed that even a simply layered structure like this can introduce complexities in the scaling of maximum ground motion with distance due to the surface wave contri-

butions. Theoretical studies of this sort should provide considerable insight for the scaling of real data.

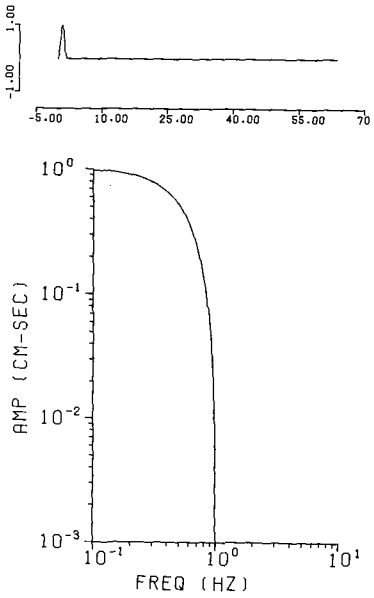

Fig. 1:

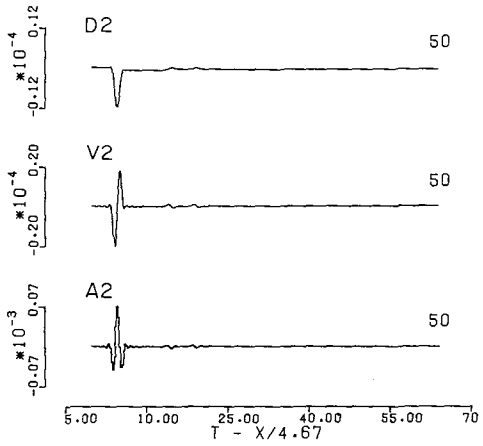

Fig.2:

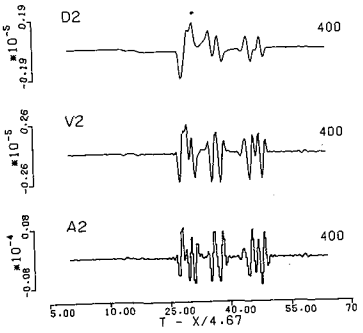

Fig. 3

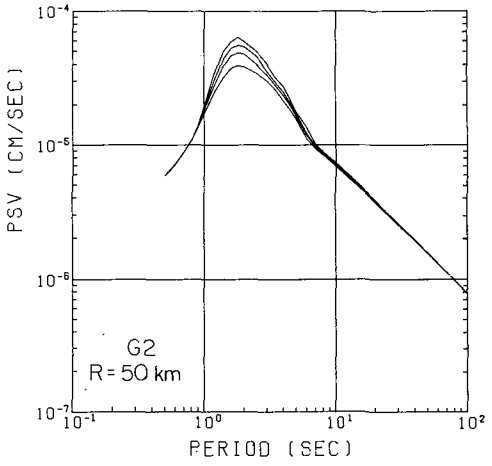

Fig. 4

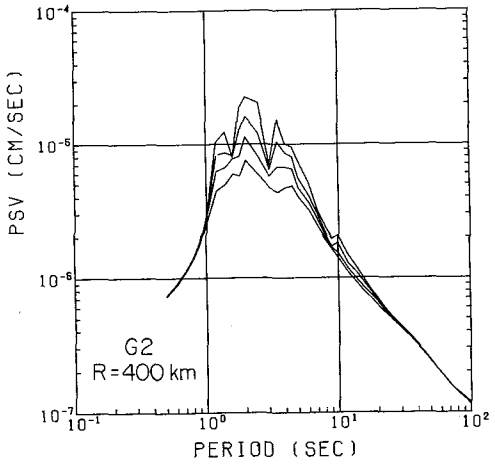

Fig. 5

REFERENCES

Herrmann, R. B., Earthquake generated SH waves in the near field and near-regional field, Misc. Paper S-77-12, Waterways Experiment Station, Vicksburg, 94, 1977.

Haskell, N. A., Radiation pattern of surface waves from point sources in a multi-layered medium, Bull. Seis. Soc. Am., 54, 377-393, 1964.

Hudson, J. A., A quantitative evaluation of seismic signals at teleseismic distances - II. Body waves and surface waves from an extended source, Geophys. J. 18, 353-370, 1969.

STATISTICS OF PULSES ON STRONG MOTION ACCELEROGRAMS

G. W. Housner

California Institute of Technology

The strong phase of an accelerogram recorded reasonably close to the causative fault, for example the 2/9/71 Holiday Inn record or the 5/18/40 El Centro record, has the general appearance of a random function with average number of zero crossings around ten per second. Between any neighbor pair of zero crossings the area under the curve represents an acceleration pulse, as regards to a building whose fundamental period of vibration is sufficiently long. For example, if the pulse has an area, A, its effect on a building would be to generate an increment of momentum $m\Delta v = A$, or an increment of velocity $\Delta v = A/m$, where m is the mass of the structure and v is the velocity. Thus, an increment of kinetic energy is imparted to the building which, in the case of a single mass structure, would be

$$\Delta KE = 1/2\ m(v + \Delta v)^2 = 1/2\ mv^2 = mv\Delta v + 1/2\ m\Delta v^2.$$

It can be expected that a pulse of area A will have an appreciably greater effect on a building than three separate pulses each of area A/3. It is, therefore, of interest to examine the statistics of pulse areas, particularly the occurrence of pulses of large areas.

Figure 1 shows the frequency distribution of pulse areas for the NS component of the 1940 El Centro earthquake (M ≈ 7), recorded approximately four miles from the surface trace of the causative fault. This is a normalized plot whose total area equals unity; that is, the original histogram was divided by the total number of pulses. The largest pulse had an area that fell between 500 and 525 mm/sec.

Figure 2 shows the frequency distribution of pulse areas for the vertical component of the 1972 Managua earthquake. The standard deviations of vertical components are always smaller than the standard deviations of horizontal components.

Figure 3 shows the frequency distribution of pulse areas (absolute values) for both horizontal components of five strong earthquake accelerograms. The records included are: El Centro 18 May 1940; Managua, 23 December 1972; Holiday Inn, 9 February 1971; Olympia, Washington, 18 April 1949; and Taft, California, 21 July 1952.

Figure 4 shows the corresponding frequency distribution for six less intense accelerograms.

The largest pulse on an accelerogram does not necessarily have the highest value of peak acceleration, which is another example of why peak acceleration is not a reliable measure of intensity of ground shaking.

There are certain difficulties in formulating a completely satisfactory definition of a pulse and relating it to the source mechanism and travel path. This makes it difficult to deduce information about pulse areas from first principals.

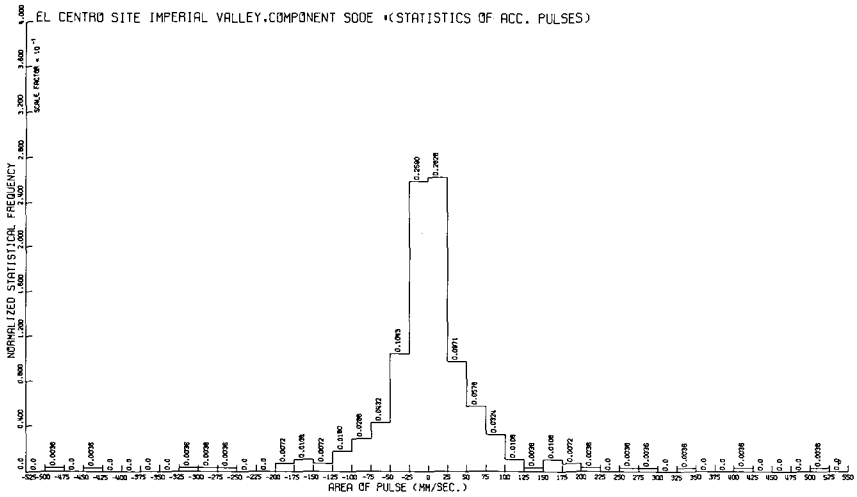
EL CENTRO SITE IMPERIAL VALLEY.COMPONENT SODE ((STATISTICS OF ACC. PULSES)
NORMALIZED STATISTICAL FREQUENCY
AREA OF PULSE (MM/SEC.)

Fig. 1

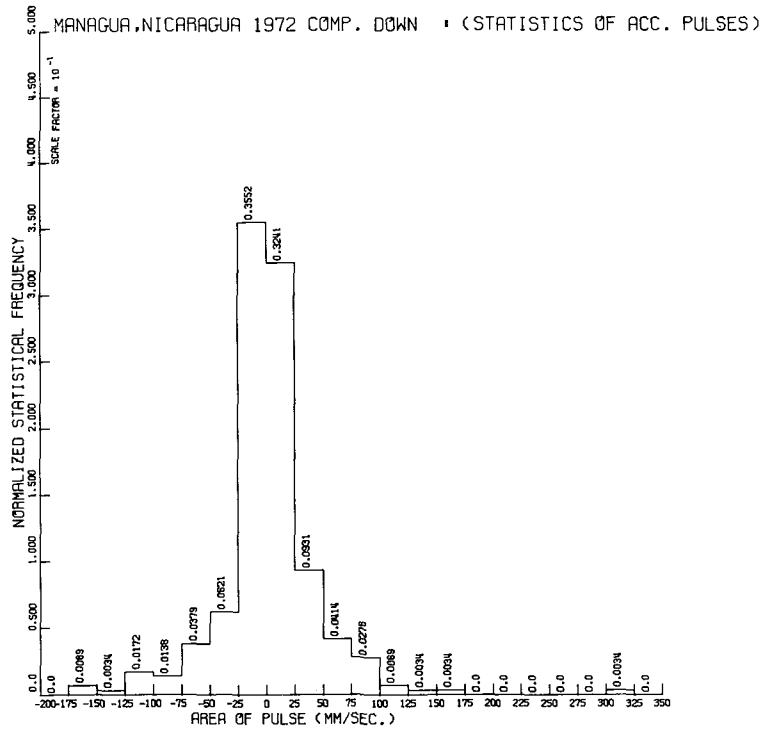
MANAGUA,NICARAGUA 1972 COMP. DOWN - (STATISTICS OF ACC. PULSES)
NORMALIZED STATISTICAL FREQUENCY
SCALE FACTOR = 10⁻¹
AREA OF PULSE (MM/SEC.)
0.0
0.0069
0.0034
0.0172
0.0138
0.0379
0.0621
0.3552
0.3241
0.0931
0.0414
0.0278
0.0069
0.0034
0.0034
0.0034

Fig. 2

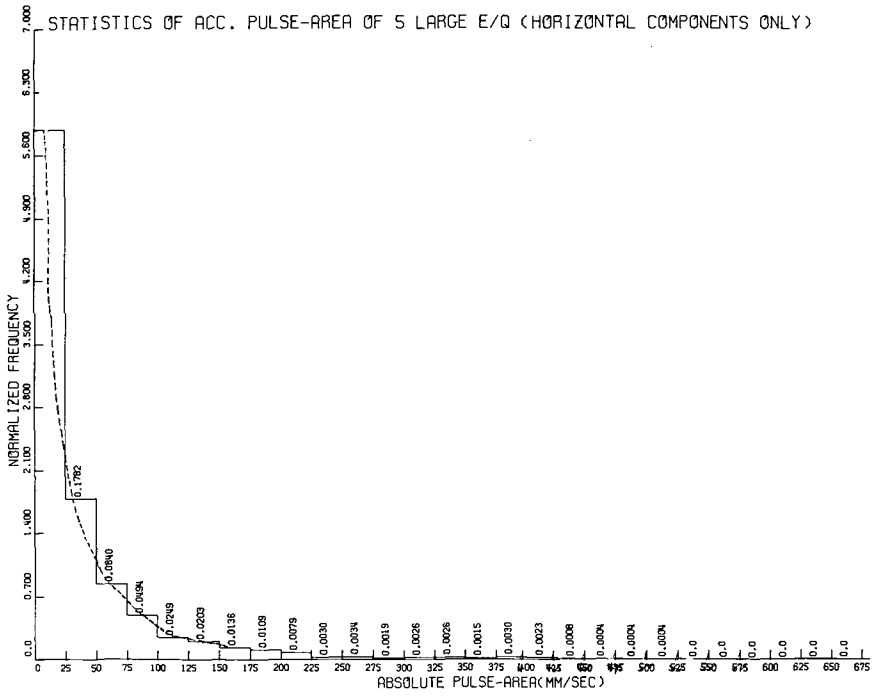
STATISTICS OF ACC. PULSE-AREA OF 5 LARGE E/Q (HORIZONTAL COMPONENTS ONLY)
NORMALIZED FREQUENCY
ABSOLUTE PULSE-AREA(MM/SEC)
0.1792
0.0840
0.0494
0.0249
0.0203
0.0136
0.0109
0.0079
0.0030
0.0034
0.0019
0.0026
0.0026
0.0015
0.0030
0.0023
0.0008
0.0004
0.0004
0.0004

Fig. 3

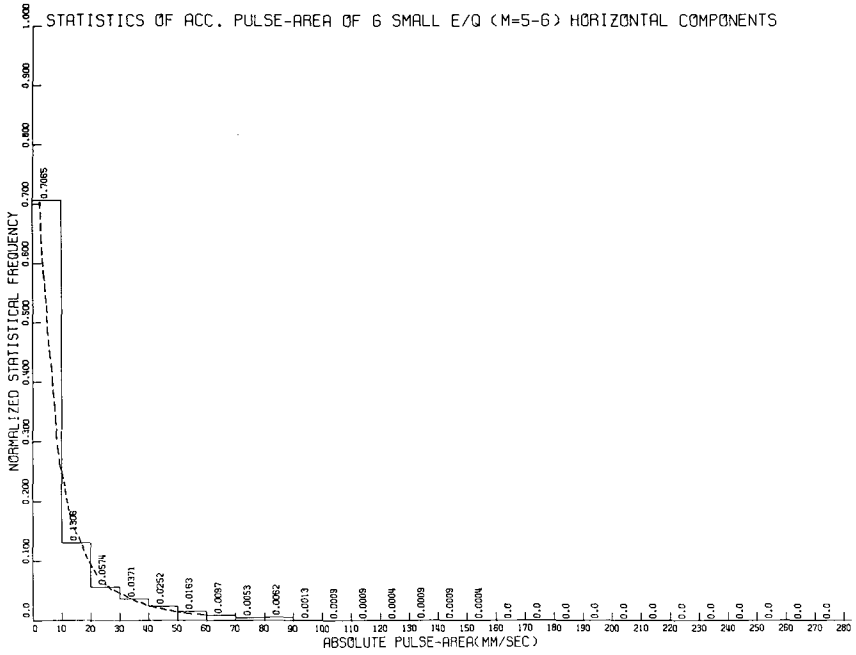
STATISTICS OF ACC. PULSE-AREA OF 6 SMALL E/Q (M=5-6) HORIZONTAL COMPONENTS
NORMALIZED STATISTICAL FREQUENCY
ABSOLUTE PULSE-AREA(MM/SEC)
0.7085
0.1396
0.0574
0.0371
0.0252
0.0163
0.0097
0.0053
0.0062
0.0013
0.0009
0.0004
0.0009
0.0009
0.0004

Fig. 4

AN INTRODUCTION TO STRONG-MOTION INSTRUMENTS AND DATA

Paul C. Jennings

California Institute of Technology

INTRODUCTION

In view of the focus of the seminar upon strong ground motion, it seemed appropriate to include in the proceedings a summary of the present status of strong-motion instruments and of programs devoted to recording strong-motion data. Also included is a brief assessment from the viewpoint of engineering of the data base of strong-motion records so far obtained.

INSTRUMENTS AND NETWORKS

Strong-Motion Instruments

The basic strong-motion instrument is the accelerograph which, in its most common form, generates a film record of three mutually perpendicular components of acceleration: vertical and two horizontal. Samples of accelerograms are shown in Figures 1 and 2. The instruments also record an internally generated time signal and reference traces. The sensitivity is commonly $\pm$1g, and the instrument is self-triggering. The basic transducer typically has a natural frequency near 25 hz and damping is of the order of 60 percent of critical. These are nominal properties of common instruments such as shown in Figure 3, and the reader is referred to the literature (e.g., 3) for properties of specific accelerographs. Although the basic instrument is the three-component accelerograph, there are a number of important variations that are becoming increasingly important in strong-motion seismology. One such instrument is the central recording accelerograph, which allows up to 12 channels of data to be recorded on a single, 7-inch film strip. This instrument is particularly useful for installation in structures and in arrays, where the small size of the transducers, which are separate from the recording mechanism, is an advantage. Another important development is the digital-recording accelerograph which has obvious advantages for data processing. Some instruments of this type have been installed in the field and records have been obtained, but not enough experience has been accumulated so far to place them in a category of reliability comparable to the film-recording systems. Another modification, of particular interest to seismology, is the addition of a timing signal. The internal timing mechanism in the instrument is supplemented by a WWVB receiver and associated electronics which results in a digitally encoded time signal on the edge of the accelerogram.

The power for the accelerometers is usually provided by batteries, which are kept at peak charge by means of slow-acting chargers connected to standard electrical outlets. Under favorable circumstances, the accelerograph will require maintenance at intervals of 6 months or longer. Under less favorable conditions, more frequent maintenance is required. About 90 to 95 percent of the accelerographs in a network can be expected to function properly with proper service. Discharged batteries and problems with the film transport system are the most common causes of difficulty.

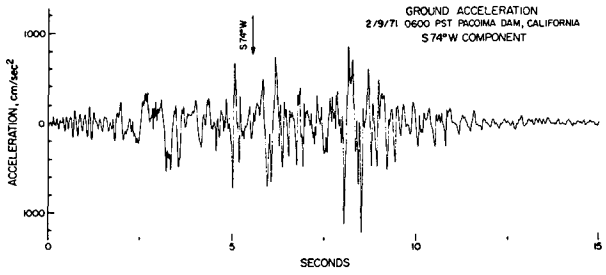

Fig. 1: S74°W component of acceleration recorded at Pacoima Dam during the San Fernando earthquake of February 9, 1971.

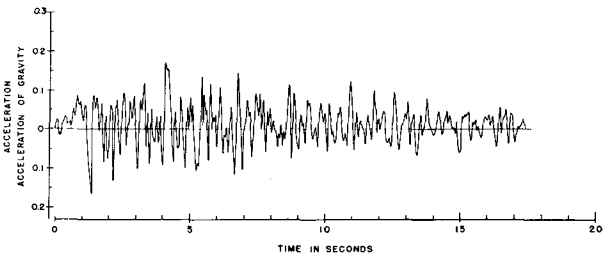

Fig. 2: S69°E component of acceleration recorded at Taft during the Kern County earthquake of July 21, 1952.

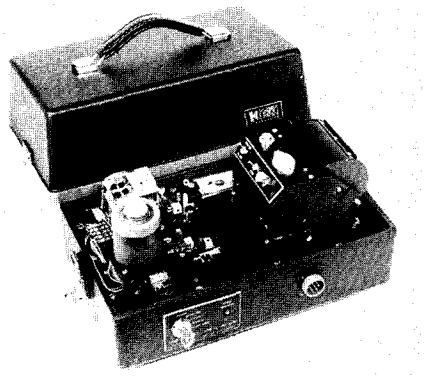

Fig. 3: SMA-1 Film-recording strong-motion accelerograph.

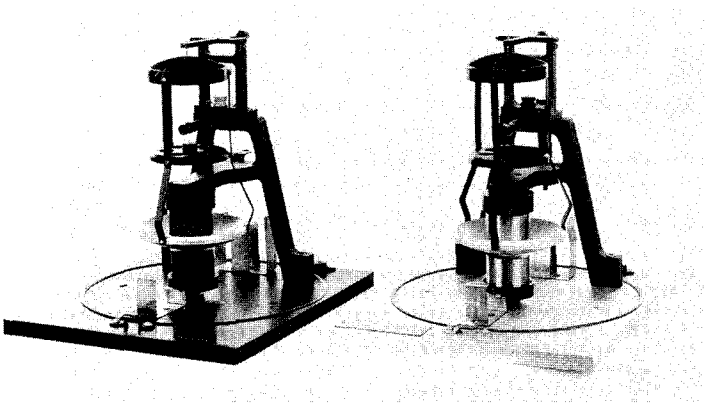

Fig. 4: Strong-motion seismoscopes. Record is scribed on smoked glass dish at top of instrument.

Another important strong-motion recorder is the seismoscope (5), illustrated in Figure 4. This instrument is basically a spherical pendulum which scratches its displacement record on a smoked watch glass, as seen in Figure 5. The natural period is commonly 0.75 second and the damping is nominally 10 percent of critical. The instrument and its properties are such that the maximum displacement can be converted to a point on the displacement response spectrum of the ground motion. Although it provides less information than the accelerograph, the seismoscope has proven to be extremely reliable and in the Guatemalan earthquake of 1976, for example, provided the only significant strong-motion record. In addition to direct reading of the instrument, there have been instances when it has been possible to estimate the history of ground acceleration from the seismoscope response, using a higher mode response of the transducer as a timing signal (12).

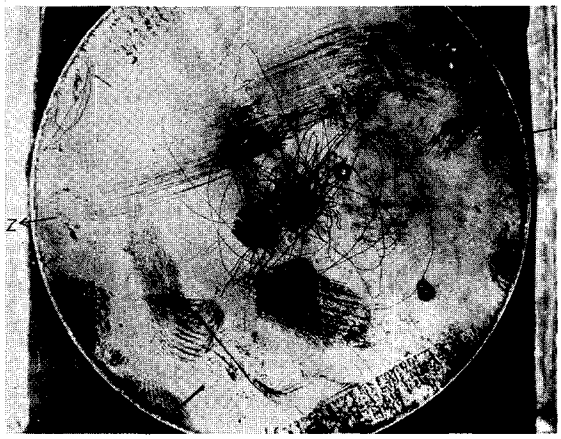

Fig. 5: Seismoscope record obtained at the University Administration building during the Guatemalan earthquake of February 4, 1976. North is to the left.

Other strong-motion instruments include such special purpose devices as peak-recording accelerographs for nuclear powerplants, Carder "displacement" meters, elevator shut-off mechanisms, and shut-off mechanisms (jiggle valves) for gas lines.

Status of Instrumental Networks

The principal agency involved in the deployment and maintenance of strong-motion instruments, and in the processing of the records obtained, is the Seismic Engineering Branch of the U. S. Geological Survey. This agency installs and maintains its own instruments and performs similar services for instruments owned by other organizations. The operating funds for the Seismic Engineering Branch are provided by the National Science Foundation under a 5-year agreement, scheduled to be renewed. Other sizeable networks are operated by the California State Division of Mines and Geology, and by the City of Los Angeles. There are additional, smaller networks operated by university research groups, utilities and other organizations. Foreign accelerograph networks exist in several countries including Japan, Mexico, Yugoslavia, Iran, Italy, New Zealand, Peoples Republic of China, and Soviet Russia among others.

As of June 1978 (9), the Seismic Engineering Branch is maintaining the following instruments under its basic program:

184 USGS accelerographs
59 accelerographs owned by other agencies
1 14-channel digital system
3 analog systems
20 accelerographs in foreign countries (chiefly South and Central America), and
1 12-channel analog system, in a foreign country.

An even larger number of accelerometers are owned by other agencies, (e.g., Corps of Engineers, U. S. Bureau of Reclamation) but are maintained by the Seismic Engineering Branch on a contract basis. This instrumentation includes:

301 accelerographs
7 installations, with a total of 72 channels of digitally-recorded data
4 installations, with a total of 38 channels of analog-recorded data.

These figures give a total of 580 installations, with approximately 1864 channels of data. The instruments are distributed thoughout the United States, with concentrations in more seismic regions.

The Seismic Engineering Branch also owns and services approximately 150 seismoscopes and maintains 25 peak recording accelerographs owned by other agencies. A few Carder displacement meters are also owned and serviced by the Branch.

The program of the California Division of Mines and Geology was established in 1972 and is operated by the Office of Strong-Motion Studies. The status of their installations, as of June 30, 1978, is summarized below (13):

Installation Type	Number	Data Channels
Surface free-field	247	741
Down-hole free-field	2	18
Buildings	35	374
Dams	16	176
Bridges	3	58
TOTALS	303	1,367

The free-field phase of the California program is approximately 50 percent completed now, and emphasis in this phase has been shifted from general distribution throughout the state toward the installation of special-purpose free-field instrumentation, including linear and down-hole arrays.

The major emphasis of the installation effort has recently been shifted to instrumentation of structures is about 10 percent complete.

The plans for the near future include instrumenting approximately 20 structures and 10 free-field sites per year, and the development of a capability for record processing and dissemination.

The City of Los Angeles maintains a network of strong-motion instruments that have been installed in tall buildings in accordance with the City Building Code. At the end of August 1977 there were 158 buildings instrumented in this program, with a total of 486 three-channel accelerographs (11). The City of Los Angeles is maintaining 143 of these buildings, while the others were maintained by other groups, including 10 serviced by the Seismic Engineering Branch.

The remaining networks of strong-motion instruments are smaller and are generally devoted to special purposes of individual groups, such as the measurement of the response of dams, the measurement of soil-structure interaction, or as complementary instrumentation for seismological research. An exception to this is the recently funded array being installed by the University of Southern California. When completed this will comprise a grid of about 90 accelerographs in the Los Angeles Basin.

The need for increased coverage by strong-motion instrumentation is recognized by all seismically active countries, and there are plans underway for an international project to install detailed arrays at selected locations in the world (7).

STRONG-MOTION DATA

Status of Strong-Motion Records

The Seismic Engineering Branch has the primary responsibility for processing, storing and disseminating strong-motion records. They do this not only for the instruments they

maintain, but also for the California Division of Mines and Geology which is in the process of developing its own data management program, the City of Los Angeles and for nearly all of the smaller, special purpose networks. They also try to obtain copies of important records obtained in foreign countries.

As of June 1978, the Seismic Engineering Branch has in its archives approximately 2800 records recorded from 750 separate events (2). With a few exceptions, each record contains three components of acceleration. Of these 2800 records about 800 are from upper stories of buildings, crests of dams, etc., leaving about 2000 records of basement or free-field motion. Approximately 100 of the 2800 records are from foreign stations. As might be expected, most of these records are of small motions and of the 2000 ground-level accelerograms only 250 are classified as being significant on the basis of having a peak acceleration of 10 percent g or more, or of being of special interest. On the same basis, some 200 of the 800 records of structural response are classified as significant.

This gives a total of about 450 significant records, with about half coming from the San Fernando earthquake. Of these 450 records, 420 have been digitized and processed and are on computer tape at the Seismic Engineering Branch in Menlo Park, The National Information Service for Earthquake Engineering (NISEE) at Berkeley and at the Environmental Data Service (EDS-NOAA) at Boulder. Copies of accelerograms can be obtained from these agencies. There is also a large file of accelerograms at the California Institute of Technology, where many of the records were digitized and processed.

In addition, there is a significant data base obtained from strong-motion recordings of aftershocks of the Oroville earthquake (4). In a period of 3 months, 313 records from 86 events were obtained from 15 stations. Of these 120 records from 14 events have been digitized. The aftershocks include records with amplitudes up to 70 percent g, although most are much smaller.

The Seismic Engineering Branch also analyzes significant seismo-scope records and archives the originals. Over 140 useable seismoscope records were obtained from the San Fernando earthquake, and a detailed report of the results has been prepared (1).

Additions to the strong-motion data, and developments in the networks are published in the program reports of the Seismic Engineering Branch (e.g., 10).

Assessment of Strong-Motion Data from the Engineering Viewpoint

The strong-motion data is fundamental to earthquake engineering. Along with the experience obtained from structural performance during earthquakes, it is the determining factor in setting the seismic design provisions of building codes and the earthquake design criteria for major engineering projects. The records of ground motion and response are also primary factors in assessing the seismic hazard of cities, in improving design practices through understanding of structural response, and in virtually all phases of earthquake engineering research.

The strong-motion data collected since the first accelerogram was obtained in the Long

Beach earthquake of 1933 have greatly increased our understanding of the potential effects of strong shaking and in general terms, our understanding is well-advanced. As engineers and seismologists, we know something about the amplitude, frequency content and duration of strong ground motion. We also have some appreciation of how these quantities are related to measures of the size of the earthquake and to the geometrical relations between source and site. There are experimental data indicating the way that strong ground motion can be affected by soil-structure interaction, by very soft soil deposits, by topography and by the presence of surface waves. We are also in a position to make meaningful estimates of some of the inherent variations that exist in strong ground shaking.

Although the general picture is encouraging, there are some very important questions for which the data are insufficient. In addition, almost none of the points described above are understood in sufficient detail, even given that complete understanding should not be expected or required for applications in earthquake engineering practice. There are two very important gaps in the data from the engineering viewpoint. First, there is a paucity of records in the near field (e.g., $\Delta < 20$ km) of major, potentially damaging earthquakes. This lack of information introduces great difficulties, and occasionally controversy, into setting the earthquake-resistant design criteria for major projects. The second major gap is the lack of strong motion records from a great (e.g., $M_S > 8$) earthquake. These earthquakes have, of course, the largest potential for disaster and knowledge of the amplitude, duration and areal extent of strong shaking is required to deal with the hazard posed by these extreme events. It should be pointed out also that there are parallel gaps in our knowledge of the response of structures to ground motions in these two categories.

There are major deficiencies in the data needed to clarify our understanding of the effects of source mechanisms, travel paths and local conditions upon strong ground motion. This is perhaps most apparent when relations between measures of the strength of ground motion (e.g., peak acceleration, peak velocity, spectral intensity) and measures of distance (e.g., epicentral distance, hypocentral distance, distance to the center of the aftershock zone) and earthquake size (e.g., local magnitude, M_L, surface-wave magnitude, M_S) are investigated. Figures 6 and 7 are plots of peak acceleration and velocity, respectively, for different magnitude classes. The figures illustrate the variability in the data and suggest the difficulty in establishing simple relations among these variables. The unsatisfactory state of present affairs is indicated by the fact that in a recent report (6), 26 different studies were identified in which relations between peak acceleration, magnitude and distance have been advanced. Clearly there is not yet a consensus on this subject. An additional feature requiring experimental clarification and verification is the effects of different source mechanisms on the strong motion. For example, theoretical studies indicate, and some data support, the concept that thrust-type earthquakes produce significantly stronger near field shaking than strike-slip events.

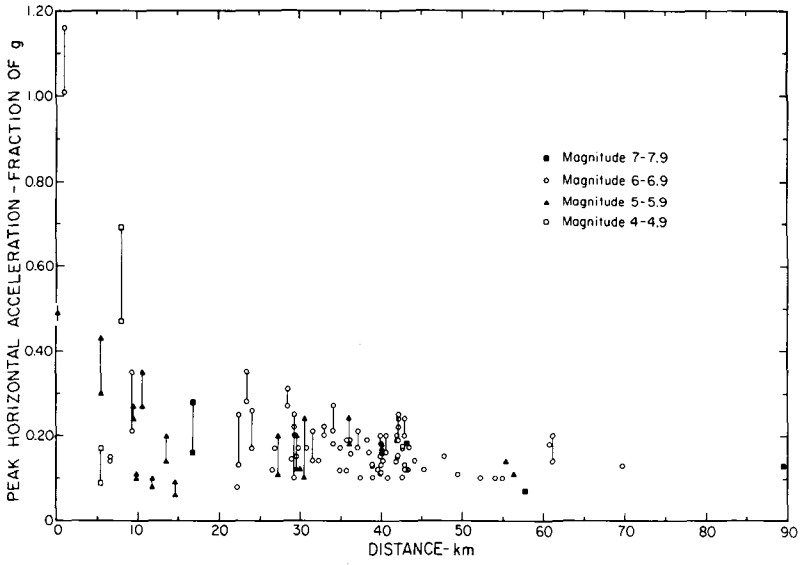

Fig. 6: Peak acceleration vs. distance for four magnitude classes. Lines join the two horizontal components of larger and closer motions.

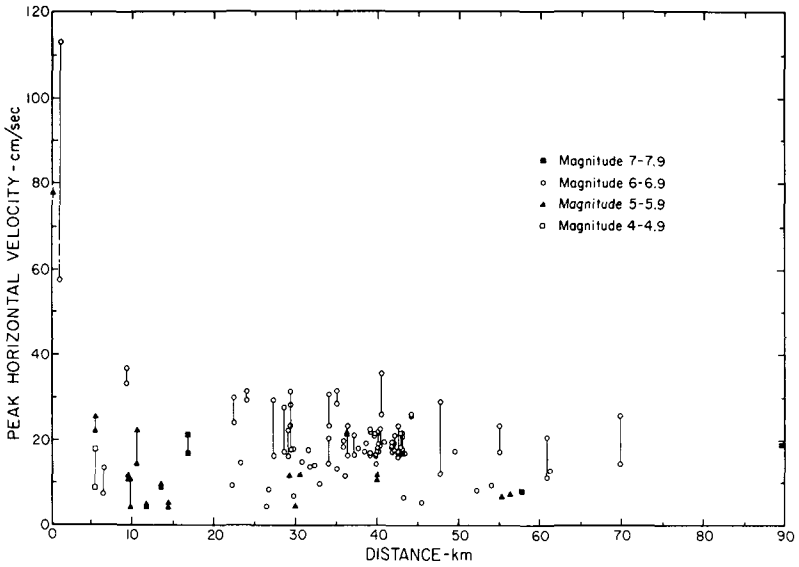

Fig. 7: Peak velocity vs. distance for four magnitude classes. Lines join the two horizontal components of larger and closer motions.

Similarly, there is no clear professional consensus on the details of how local site conditions can affect strong ground motion. Although there is general agreement on the qualitative nature of such effects, there is a divergence of judgements on the degree of the effects as seen in the data, the role of surface waves, and the degree to which engineering solutions can be reliably obtained from analyses of simplified models of the phenomenon. More strong-motion data clearly are required to further the understanding of the potential effect of local conditions on the ground motions, and several of the strong-motion arrays now being installed are designed to yield some of this data.

Additional strong-motion data are also needed to clarify the role of soil-structure interaction in modifying the earthquake motion transmitted to the structure. The interaction problems include the effects of the compliance of the foundation, the effects of embedment, and the effects of foundations with large areas in suppressing motions of high frequency. Some instrumental arrays now installed will provide records bearing on these problems, but improvement is needed. For example, the effects of large foundations on high frequency motion appear to be quantitatively similar to effects soft soils are thought to have on these motions. In the very common case of a record obtained in the base of a sizeable building

founded on fairly soft alluvium, it may not be possible to separate the two effects without additional instrumentation.

Finally, it should be stated that the strong-motion data base is insufficient to determine the variability in strong ground motion under specified circumstances. The problem arises, for example, when the level of the mean plus one standard deviation is sought for the expected response spectra at a site of a nuclear power plant. Different investigations of the existing data and different approaches to the assessment of the variability can lead to significantly different results, with large economic implications for the project.

ACKNOWLEDGEMENT

The above discussion was taken with minor modification from the paper "Strong-Motion Seismology" (8) which the author and Donald V. Helmberger prepared for presentation at the second International Conference on Microzonation, held in San Francisco, November 26 - December 1, 1978.

REFERENCES

1. Borrill, B. J., Seismoscope results -- San Fernando earthquake of 9 February 1971, Chapter 3 of Strong-Motion Instrumental Data on the San Fernando Earhtquake of February 9, 1971, D. E. Hudson (Ed.), Earthquake Engineering Research Laboratory, California Institute of Technology, and Seismological Field Survey, National Oceanic and Atmospheric Administration, U. S. Department of Commerce, Pasadena, California.
2. Brady, A. G., Personal communication, 1978.
3. Halverson, H., A technical review of recent strong motion accelerographs, Proceedings of the Fifth Work Conference on Earthquake Engineering, I, 1046-1055, Edigraph, Rome, 1974.
4. Hanks, T. C. and L. C. Seekins, Strong motion accelerograms of the Oroville aftershocks and peak acceleration data, Bull. Seism. Soc. Am., 68, No. 3, 677-689, 1978.
5. Hudson, D. E. and W. K. Cloud, A simplified instrument for recording strong motion earthquakes, Bull. Seism. Soc. Am., 51, 159-174, 1961.
6. Idriss, I. M., State of the art -- ground motions, presented at the ASCE Earthquake Engineering and Soil Dynamics Conference and Exhibit, Pasadena, California June 19-21, 1978.
7. Iwan, W. D. (Ed.), Proceedings of the International Workshop on Strong Motion Earthquake Instrument Arrays, Honolulu, May 2-5. Earthquake Engineering Laboratory, California Institute of Technology, 1978.
8. Jennings, P. C. and D. V. Helmberger,"Strong-Motion Seismology" presented at the second International Conference of Microzonation, San Francisco, November 26 - December 1, 1978. (To appear in the conference proceedings)
9. Maley, R. P., Personal communication, 1978.
10. Porcella, R. L. (Ed.), Seismic engineering program report, September - December 1977, Geological Survey Circular 762-C, 1978.
11. Robb, J. O., Personal communication, 1978.

12. Scott, R. F., The calculation of horizontal accelerations from seismoscope records, Bull Seism. Soc. Am., 63, No. 5, 1637-1661, 1973.

13. Wooten, T.M., Personal Communication.

THE APPLICATION OF SYNTHETIC SEISMOGRAMS TO THE STUDY OF STRONG GROUND MOTION

Lane R. Johnson
University of California, Berkeley

Donald V. Helmberger
California Institute of Technology

The factors affecting strong ground motion during earthquakes can be divided into three main areas: the source mechanism, wave propagation effects, and local site geology. In order to interpret available strong motion data or make projections to strong motions that can be expected during future earthquakes, it is important to understand how each of these factors contributes to the strong motion. In this study, we have used a suite of synthetic seismograms to arrive at some general conclusions concerning the effects that the source mechanism and propagation have upon strong ground motion.

The basic dislocation model of an earthquake source (*Burridge and Knopoff*, 1964, *Haskell*, 1964, *Haskell*, 1969, *Savage*, 1966), is most commonly used for the purposes of modeling strong ground motion. The effects of wave propagation are normally handled by calculating an appropriate Green's function and efficient methods for doing this are available (*Ben-Menahem*, 1973, *Helmberger*, 1974, *and Johnson*, 1974). The combination of the source model and the Green's function yields a synthetic record of the ground motion. Several studies have demonstrated that reasonable assumptions about the mechanics of the source and the physical properties of the crust lead to synthetic seismograms that closely approximate observed strong ground motion records (*Heaton and Helmberger*, 1977, *Helmberger and Johnson*, 1977, *Helmberger and Malone*, 1975, *Israel and Vered*, 1977, *Johnson and McEvilly*, 1974, *Savage*, 1966).

Starting with the premise that synthetic seismograms have been used successfully to interpret specific records of strong ground motion, the objective of this study was to determine what general conclusions about strong motion could be obtained from a systematic examination of synthetic seismograms. Synthetic seismograms were calculated in the epicentral range of 4 to 128 km from a point dislocation source buried 8 km deep in a homogeneous elastic crust 32 km thick. In the sense that this is an oversimplified model for a realistic earthquake, the results serve as a lower bound on the complexity to be expected in realistic ground motion.

At distances less than about four source depths, the synthetic strong motion records are dominated by the direct P and S waves and the refracted sP wave. The near-field parts of the elastodynamic solution are also prominent and affect primarily the interpretation of the longer periods of ground motion. At distances beyond about one crustal thickness, the effect of the crust-mantle boundary becomes important and contributes to the complexity and duration of ground motion.

Representative results are shown in Figure 1 which contains synthetic records of ground displacement in the horizontal direction from a strike-slip type source. The transition from a record dominated by body waves to one dominated by surface waves is clear. The large number

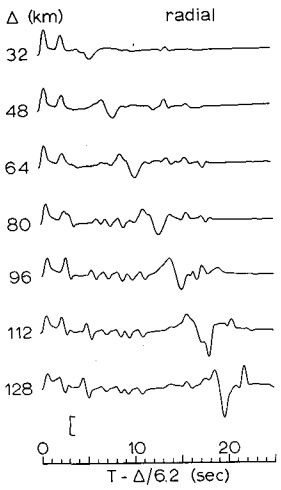

Fig. 1

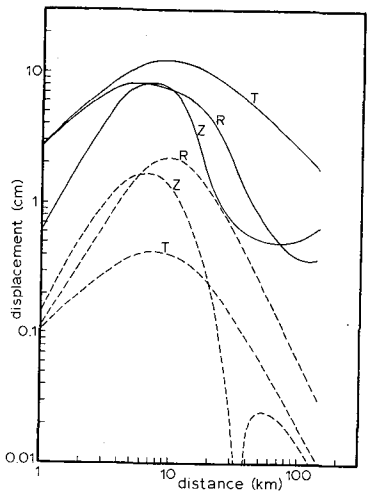

Fig. 2

of reflected and refracted waves with significant amplitudes is also noteworthy. For instance, at a distance of 100 km, 26 different possible waves are predicted for the first 20 sec. of the record. The controlling criteria for the amplitudes of these waves are the radiation pattern of the source and whether the distance is sufficient so that reflections take place beyond critical angles.

Figure 2 summarizes the dependence of amplitude upon distance for the same type of source. The maximum dynamic displacements are roughly constant for distances less than about one source depth and exhibit a dependence that varies between $(\text{distance})^{-1/2}$ and $(\text{distance})^{-2}$ at greater distances. The static displacements show a similar behavior except that the dependence varies between $(\text{distance})^{-2}$ and $(\text{distance})^{-3}$ at large distances. At distances of about one source depth the ratio between the maximum dynamic and static displacements can be less than 5.

REFERENCES

Ben-Menahem, A. and M. Vered, Extension and interpretation of the Cagniard-Pekeris method for dislocation sources, Bull. Seis. Soc. Am., 63, 1611-1636, 1973.

Burridge, R. and L. Knopoff, Body force equivalents for seismic dislocations, Bull. Seis. Soc. Am., 54, 1875-1888, 1964.

Haskell, N. A, Total energy and energy spectral density of elastic wave radiation from propagating faults, Bull. Seis. Soc. Am., 54, 1811-1841, 1964.

Heaton, T. H. and D. V. Helmberger, A study of the strong ground motion of the Borrego Mountain, California, earthquake, Bull. Seis. Soc. Am., 67, 315-330, 1977.

Helmberger, D. V., Generalized ray theory for shear dislocations, Bull. Seis. Soc. Am., 64, 45-64, 1974.

Helmberger, D. V. and L. R. Johnson, Source parameters of moderate size earthquakes and the importance of receiver crustal structure in interpreting observations of local earthquakes, Bull. Seis. Soc. Am., 67, 301-313, 1977.

Helmberger, D. V. and S. D. Malone, Modeling local earthquakes as shear dislocations in a layered half-space, J. Geophys. Res., 80, 4881-4888, 1975.

Johnson, L. R., Green's function for Lamb's problem, Geophys. J. R. Astr. Soc., 37, 99-131, 1974.

Johnson, L. R. and T. V. McEvilly, Near-field observations and source parameters of central California earthquakes, Bull. Seis. Soc. Am., 64, 1855-1886, 1974.

Savage, J. C., Radiation from a realistic model of faulting, Bull. Seis. Soc. Am., 56, 577-592, 1966.

Vered, M. and A. Ben-Menahem, Application of synthetic seismograms to the study of low-magnitude earthquakes and crustal structure in the northern Red Sea region, Bull. Seis. Soc. Am., 64, 1221-1237, 1974.

SEMI-EMPIRICAL APPROACH TO PREDICTION OF GROUND MOTIONS PRODUCED BY LARGE EARTHQUAKES

Hiroo Kanamori

California Institute of Technology

PROCEDURE FOR THE SYNTHESIS OF LONG-PERIOD GROUND MOTIONS PRODUCED BY GREAT EARTHQUAKES

We are primarily concerned with very long period (several seconds or longer) ground motion generated by a great earthquake, expecially by a long transcurrent fault earthquake such as the 1906 San Francisco or 1857 Fort Tejon earthquakes. Recent studies indicate that most large earthquakes (e.g., *Imamura*, 1937; *Wyss and Brune*, 1967; *Trifunac and Brune*, 1970) are complex multiple events. For example, the 1976 Guatemalan earthquake (Kanamori and Stewart, 1978, see Figure 1) can be modeled by approximately 10 events with $M_S \simeq 6.5$ (fault length 10 to 20 km) which occurred in sequence along the fault. Thus the ground motion from this type of earthquake may be predicted by convolving the ground motion of the individual event with the source function describing the space-time history of the multiple shock sequence. Recent seismological studies have shown that for this period range, the ground displacement caused by moderate size (fault-length $\lesssim$ 20 km) earthquakes can be predicted by a simple dislocation model (e.g. *Aki*, 1968; *Kanamori*, 1972; *Mikumo*, 1973; *Trifunac*, 1974; *Abe*, 1974a,b,1975 *Helmberger and Malone*, 1975; *Burdick and Mellman*, 1976; *Langston*, 1976; *Langston and Butler*, 1976; *Heaton and Helmberger*, 1977; *Heaton and Helmberger*, 1978). Since the individual event of the Guatemala earthquake is probably small enough to be modeled by a simple dislocation model, the above procedure may be useful for predicting long period ground motions produced by a large earthquake.

A more empirical approach may also be used as follows. For the Guatemala earthquake, the individual event is very similar to the 1968 Borrego Mountain earthquake, for which a detailed source model has been determined (*Burdick and Mellman*, 1976; *Heaton and Helmberger*, 1977). A recent analysis of strong motion and seismoscope records (*Kanamori and Jennings*, 1978; *Jennings and Kanamori*, 1978) suggests that the Guatemala earthquake and the Borrego Mountain earthquake have about the same M_L (local magnitude) indicating that the Borrego Mountain earthquake and the individual event of the Guatemala earthquake are of about the same size at periods around 1 sec. This result suggests that long period ground motions produced by a Guatemala type earthquake may be empirically predicted by convolving the appropriately scaled ground motion produced by the Borrego Mountain earthquake with the source time sequence of the Guatemala earthquake.

ESTIMATION OF THE MAXIMUM AMPLITUDE OF STRONG MOTION FROM THE LOCAL MAGNITUDE M_L

Despite the recent progress in seismology, it is still very difficult to predict short-period (eg., less that 2 sec.) ground motion by using existing methods. One possible approach to this problem is to use the local magnitude, M_L. The local magnitude, M_L, has direct rele-

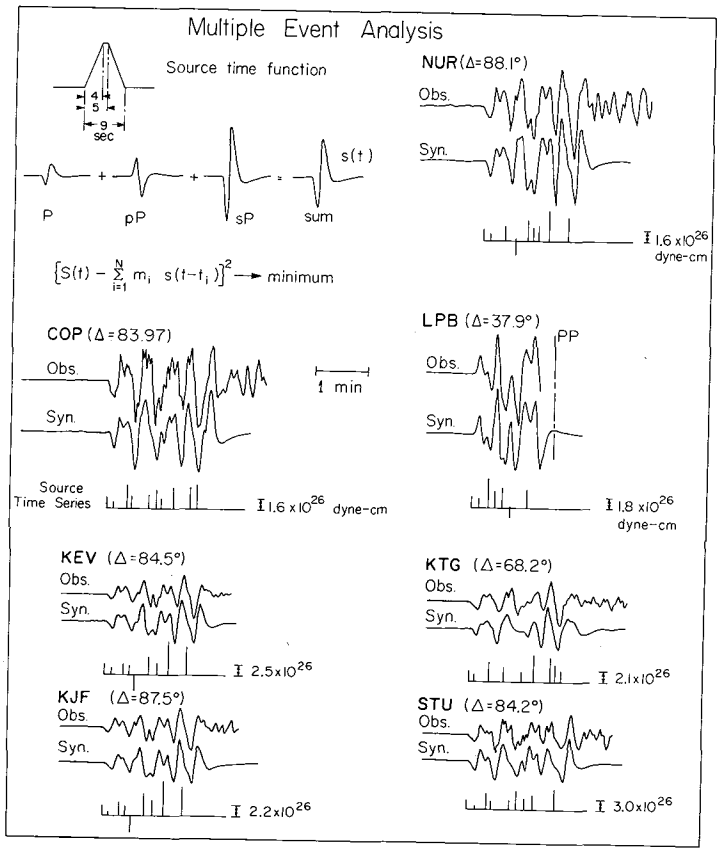

Fig. 1: Observed and synthetic P waves for individual WWSSN stations obtained from the multiple shock analysis. For each station the source time series is obtained using the source time function shown here. The surface reflections pP and sP are included in the source time function. The resulting series is given for each station along with the moment for the first event. The height of the vertical bar is proportional to the moment of the individual event. Δ is the epicentral distance.

vance to engineering applications because M_L is determined within the period range of greatest engineering interest (0.3 to 2 sec.). However, M_L has been traditionally determined by using high gain seismographs (e.g., the Wood-Anderson seismograph). Hence, most of the records of very large earthquakes go off scale at short distances precluding their use in determining M_L. For large earthquakes ($M_L \geq 5.5$), M_L is determined only at large distances. Since correction for the decay of the amplitude as a function of distance is incorporated in the M_L scale, the values of M_L should not depend upon the distance. However, the amplitude-distance curve used in the M_L scale is calibrated by using small earthquakes so that it is not clear whether it also applies to very large earthquakes.

It is possible that, for very large earthquakes, complex interference of seismic waves originating from different parts of the fault plane may significantly affect the decay rate of the maximum amplitude resulting in distance dependent M_L.

Recently, *Kanamori and Jennings* (1978) showed that strong motion accelerograms can be used to calculate a synthetic Wood-Anderson response by which M_L can be determined at short distances (see Figure 2).

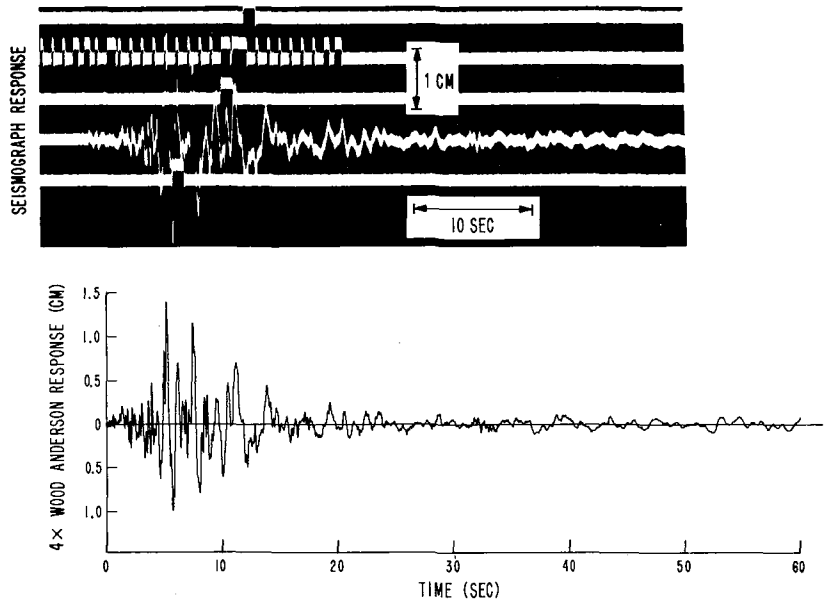

Fig. 2: Comparison of the record observed by a 4X torsion seismograph (upper trace) with the 4X Wood-Anderson response calculated from the strong-motion record. The records are the N-S component of the 1971 San Fernando earthquake obtained at the Seismological Laboratory at the California Institute of Technology.

Figure 3 shows the value of M_L as a function of distance for several California earthquakes. All the data points are obtained from M_L determined from strong-motion accelerograms. Although data are not complete, there is no obvious dependence of M_L on distance suggesting that the amplitude decay curve currently used is applicable to these large earthquakes. If this is the case, the value of M_L = 7.2 for the Kern County earthquake would predict a maximum amplitude on Wood-Anderson records of 440 m at a distance of 10 km from the epicenter which suggests an amplitude, velocity, and acceleration of ground motion of 25 cm, 2 m/sec., and 1.58 g respectively, if a predominant period of 0.8 sec. is assumed (see Figure 4). Because of the lack of close-in strong motion data from very large earthquakes, the above result should be considered tentative. However, this approach, when more close-in data are obtained, will provide a useful estimate of the maximum ground motion on the basis of seismological consideration.

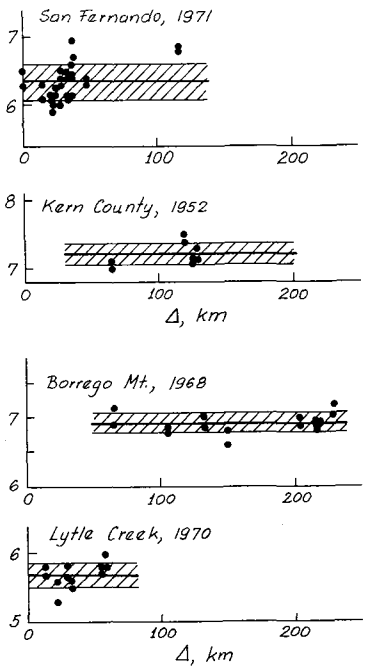

Fig. 3: M_L as a function of distance for several California earthquakes. The hatched zone indicates the mean ± one standard deviation.

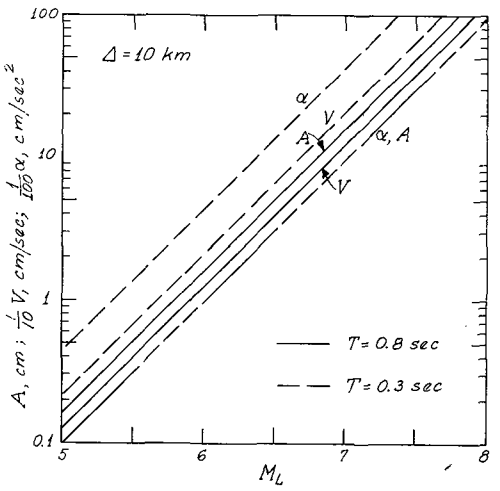

Fig. 4: The maximum displacement A, velocity V, and acceleration α at a distance of 10 km as a function M_L. The solid lines are for a period of 0.8 sec. and the dashed lines are for a period of 0.3 sec.

REFEREMCES

Abe, K., Seismic displacement and ground motion near a fault: The Saitama earthquake of September 21, 1931, J. Geophys. Res., 79, 4393-4399, 1974a.

Abe, K., Fault parameters determined by near- and far-field data: The Wakasa bay earthquake of March 26, 1963, Bull. Seis. Soc. Am., 64, 1369-1382, 1974b.

Abe, K., Static and dynamic parameters of the Saitama earthquake of July 1, 1968, Tectonophysics, in press, 1975a.

Aki, K., Seismic displacement near a fault, J. Geophys. Res., 73, 5359-5376, 1968.

Burdick, L. J., and G. R. Mellman, Inversion of the body waves from the Borrego Mountain earthquake to the source mechanism, Bull. Sesi. Soc. Am., 66, 1485-1499, 1976.

Heaton, T. H., and D. V. Helmberger, A study of the strong ground motion of the Borrego Mountain, California earthquake, Bull. Seis. Soc. Am., 67, 315-330, 1977.

Heaton, T. H., and D. V. Helmberger, Predictability of strong ground motion in the Imperial Valley, Bull. Seis. Soc. Am., in press, 1978.

Helmberger, D. V., and S. D. Malone, Modeling local earthquakes as shear dislocations in a layered half space, J. Geophys. Res., 80, 4881-4888, 1975.

Imamura, A., Theoretical and Applied Seismology, Maruzek, Tokyo, 358, 1937.

Jennings, P. C., and H. Kanamori, Determination of local magnitude, M_L, from seismoscope records, in preparation to be submitted to Bull. Seis. Soc. Am., 1978.

Kanamori, H., Determination of effective tectonic stress associated with earthquake faulting-Tottori earthquake of 1943, Phys. Earth Planet. Interiors, 5, 426-434, 1972.

Kanamori, H., and G. S. Stewart, Seismological aspects of the Guatemala earthquake of Feb. 4, 1976, J. Geophys. Res., in press, 1978.

Kanamori, H., and P. C. Jennings, Determination of local magnitude, M_L, from strong motion accelerograms, Bull. Seis. Soc. Am., in press, 1978.

Langston, C. A., A body wave inversion of the Koyna, India earthquake of December 10, 1967, and some implications for body wave focal mechanisms, J. Geophys. Res., 81, 2517-2529, 1976.

Langston, C. A., and R. Butler, Focal mechanism of the August 1, 1975, Oroville earthquake, Bull. Seis. Soc. Am., 66, 1111-1120, 1976.

Mikumo, T., Faulting process of the San Fernando earthquake of February 9, 1971 inferred from static and dynamic near-field displacements, Bull. Seis. Soc. Am., 63, 249-269, 1973.

Trifunac, M. D., A three-dimensional dislocation model for the San Fernando, California earthquake of February 9, 1971, Bull. Seis. Soc. Am., 64, 149-172, 1974.

Trifunac, M. D., and J. N. Brune, Complexity of energy release during the Imperial Valley, California, earthquake of 1940, Bull. Seis. Soc. Am., 60, 137-160, 1970.

Wyss, M., and J. Brune, The Alaska earthquake of 28 March 1964: A complex multiple rupture, Bull. Seis. Soc. Am., 57, 1017-1023, 1967.

DETERMINISTIC MODELING OF SOURCE MECHANISMS UTILIZING NEAR- AND FAR-FIELD SEISMIC DATA: THE 1971 SAN FERNANDO EARTHQUAKE

Charles A. Langston

Pennsylvania State University

Depending on frequency band, instrument characteristics, distance from source, and other factors, seismic radiation from earthquakes is categorized in many ways by both geophysicists and engineers. As a result of this data division, inversions for source processes and geometry through application of deterministic models often do not utilize the possible constraints which may occur in other data categories. Rather, many studies are very restrictive and apply a particular model or modeling technique to a limited data subset, thereby increasing uniqueness problems. Recognizing that non uniqueness is the greatest problem in all geophysical studies, it therefore seems reasonable to adopt a more global modeling concept in which the earthquake and its physical processes assume the central focus. Models for the earthquake must satisfy all observed data or must otherwise be discarded. An efficient way to arrive at a model or set of models is to examine as much of the data as possible to determine a set of constraints.

With this philosophy in mind, teleseismic P, SV, and SH waves recorded by the WWSS and Canadian networks from the 1971 San Fernando earthquake were modeled in the time domain to determine detailed features of the source as a prelude to studying the near and local field strong motion observations. Synthetic seismograms were computed from the model of a propagating finite dislocation line source imbedded in layered elastic media. The effects of source geometry and directivity were found to be important features of the long period observation. The most dramatic feature of the model was the requirement that the fault, which initially ruptured at a depth of 13 km as determined from pP-P times, continuously propagated towards the free surface, first on a plane dipping 53°NE, then broke over to a 29°NE dipping fault segment. This effect is clearly shown in the azimuthal variation of both long period P and SH waveforms. Figure 1 shows observed (top) and synthetic (bottom) P waveforms at 17 WWSS and Canadian network stations for the final inferred fault model. The P first motion plot is represented by the equal area projection of the lower half of the focal sphere. The nodal planes are for the bottom (solid lines) and top (dashed lines) sections of the final fault model. Note the prominent dilatational arrival approximately 10 seconds into the P waveforms for stations in the northern and western azimuths. This arrival, which disappears for stations in eastern and southern azimuths, is interpreted to be the combined effect of P, pP, and sP from the top section of the San Fernando Fault.

Figure 2 demonstrates the good sensitivity that the long period data have for some of the model parameters. Comparisons of theoretical waveforms with representative observed P,

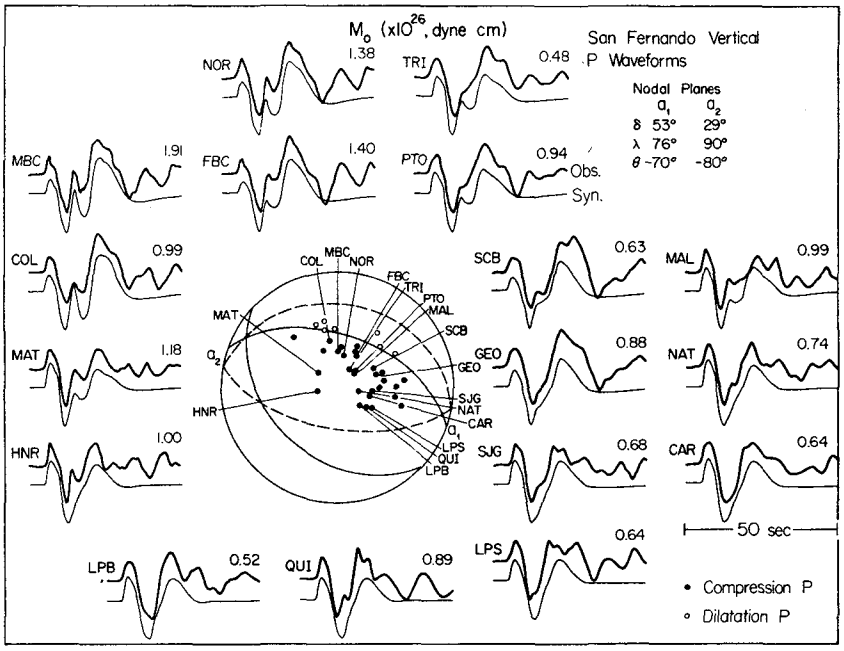

Fig. 1

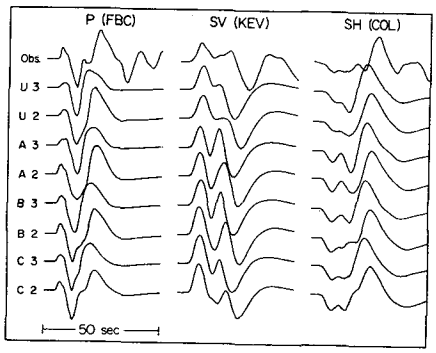

Fig. 2

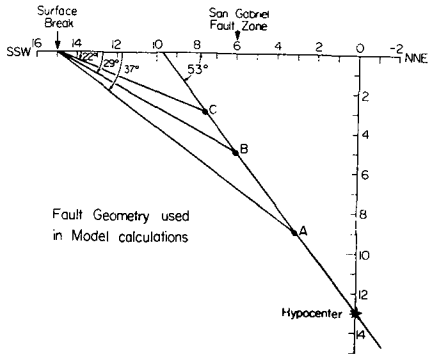

Fig. 3

SV, and SH waveforms are shown. The first letter of each model represents the fault geometry shown in Figure 3. Geometry U is unilateral rupture from the hypocenter to the free-surface on the 53° dipping plane. A, B, and C designate fault plane breakover points at 9, 5, and 3 km depths, respectively. The values 3 and 2 after each letter indicate rupture velocity in km/sec. Rupture starts at 13 km depth and propagates up the fault. Figure 2 demonstrates that wave duration and relative peak timing are closely related to rupture velocity. Relative amplitudes in each waveform indicate orientation. From similar model comparisons with all the data, the average rupture velocity from hypocenter to surface is constrained to be, at most, 1.8 km/sec.

Results from analysis of teleseismic short period P waves suggest further constraints on the nature of the initial rupture. Although attenuation and interference with radiation from the fault are possible, complications, comparison of long and short period P, and short period pP and P waves suggest that rupture was initially bilateral, or possibly, strongly unilateral downwards, propagating to about 15 km depth. Figure 4 condenses the results of many modeling experiments performed to explain the anomalously large short period P to pP amplitude ratio. For the orientation determined from a well constrained long period fault plane solution, pP should be as large or larger in amplitude as P for a point source or unilaterally upward pro-

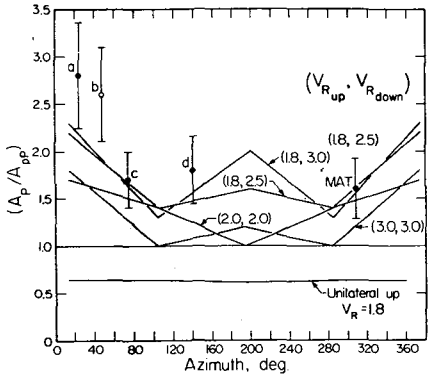

Fig. 4

pagating rupture. Points shown in Figure 4 are P-pP amplitude ratios taken from a stacking procedure and corrected for radiation pattern and the free-surface reflection coefficient. Lines are expected amplitude ratios for models in which the rupture velocity was allowed to differ for updip and downdip directions around the hypocenter. The best agreement occurs for those models in which rupture is faster downward. Long period P-short period P wave amplitudes do not discriminate between these models well, except for ruling out the simple unilaterally upward propagation.

These geometrical and dynamical constraints determined from teleseismic waveshape and amplitude data are not totally met by any previous model determined from dynamic near-field data. The complication of initial faulting occurring bilaterally or unilaterally downwards qualitatively affects understanding of the initiation of faulting and state of stress in hypocentral region. Of course, these simple models for the teleseismic data must be further modified as other constraints are determined from near-field dynamical models and other data in an iterative procedure. It is hoped that future studies of source processes and mechanisms will incorporate more diverse sources of data with greater effort to reduce uniqueness problems.

SELECTED REFERENCES

Langston, C. A., and D. V. Helmberger, A Procedure for Modeling Shallow Dislocation Sources, Geophys. J. R. astr. Soc. 42, 117-130, 1975.

Langston, C. A., The February 9, 1971 San Fernando Earthquake: A Study of Source Finiteness in Teleseismic Body Waves, Bull. Seis. Soc. Am. 68, 1978.

OCCURRENCE OF STRONG GROUND MOTIONS

R. B. Matthiesen
USGS, Menlo Park, CA

The availability of data from several stations at which strong motion accelerographs have been installed for about 40 years provides for a direct evaluation of the "recurrence" of strong ground motions at those sites. The records obtained from the site at Hollister, which was installed in 1944, are used for illustration. In Figure 1 the cumulative number of events for which peak accelerations exceeded four selected values are plotted vs the year in which the event occurred. Similar results can be obtained for each value of peak acceleration recorded at the site. The slopes of the "best fit" straight lines define the "events per year" for each value of peak acceleration, whereas the deviations from the straight lines indicate the extent to which the concept of "recurrence" is not applicable. No attempt has been made to distinguish between foreshocks, mainshocks, and aftershocks in compiling these data, so that clustering of the data may be an indication of foreshock or afterschock activity associated with a mainshock. Obviously, the inclusion of such data influences the interpretation of the final results.

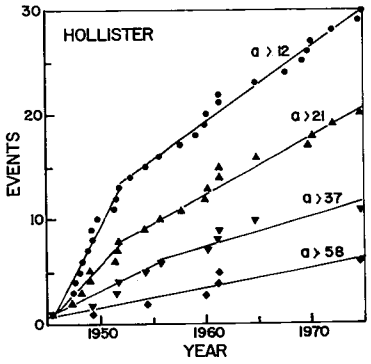

Fig. 1

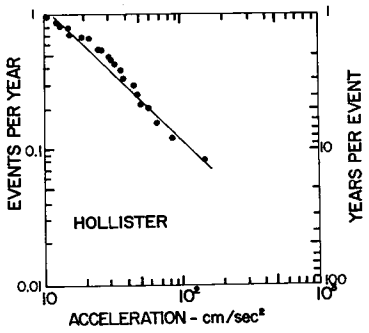

Fig. 2

The "events per year" as obtained from the slopes of the "best fit" lines can be plotted vs each successive value of recorded peak acceleration to obtain a "recurrence" curve as shown in Figure 2. Thus, the four sets of data shown in Figure 1, which were selected for illustration, represent only four of the data points shown in Figure 2. The slope of the "recurrence" line indicates a "b" value of about -1.0, which is in agreement with values obtained from regional recurrence studies (see *Algermissen and Perkins*, 1976, for example). Similar studies were made for 21 other sites. In seven cases, the recurrence curves indicate

"b" values of about -1.0, but only in three cases is there sufficient data to place some confidence in the results. Furthermore, it is significant that for 14 sites at which strong motion accelerographs have been installed for more than forty years, the amount of data is not sufficient to define recurrence curves.

In order to extend this study of recurrence of strong ground motions to other sites, the occurrence of MMI = VI or greater events have been evaluated for selected sites in regions of relatively high activity. The data set used in the evaluation was the compilation by *Coffman and von Hake* (1973). This is believed to be a reasonably consistent set for most of the country for the period from 1870 to 1970, although no such compilation can be expected to be uniformly consistent, complete, or totally accurate. Only events of MMI = VI or greater have been considered since lower intensities are associated with ground motions below the threshold of significant strong ground motion (say, a maximum ground acceleration of 0.05 g). For each event was approximated as a circle drawn around the epicenter, as illustrated in Figure 3. On these maps the areas in which several strong-motion records could have been obtained are indicated by the overlapping of the circles, and the number of events that would have caused significant ground motions at a particular site can be determined by counting the number of times that the site is encircled by the MMI = VI contours.

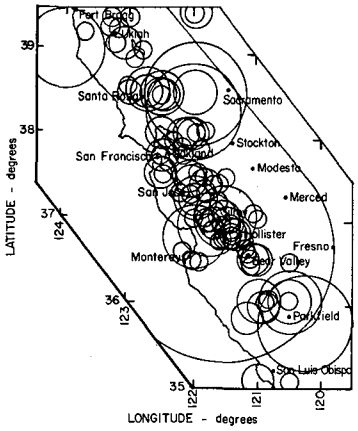

Fig. 3

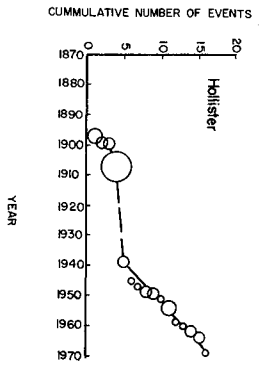

Fig. 4

By identifying the events associated with the MMI = VI contours encircling a site, a history of possible strong-motion recording at any specific site may be projected, and the cumulative number of events vs the date of projected recording may be plotted. If the concept of "recurrence" has meaning, such projected histories should indicate a linear relation between the number of events and the date of occurrence. The projected history at Hollister

is shown in Figure 4. This is in agreement with the actual history of strong motion recording at the site since 1940, but indicates a quiescent period from 1906 to 1940. Hollister is near the southern end of the 1906 fault rupture. This suggests that the state of stress in the Hollister area was relieved by the 1906 event and that the present rate of 4 years per event is "back to normal".

This brief study of the occurrence of strong ground motions indicates that the concept of "recurrence" applies in a limited sense to many sites, but when looked at with a jaundiced eye the conclusions are the same as those stated by *McGuire* (1977): "...the most recent past is the best indicator of seismic activity in the near future, ...", but "... a large amount of data cannot be indiscrinimately thrown together to calculate a mean activity rate.."

REFERENCES

Algermissen, S. T. and D. M. Perkins, A Probabilistic Estimate of Maximum Acceleration in Rock in the Contiguous United States, USGS, Open File Report 76-416, 1976.

Coffman, J. L. and C. A. von Hake, Earthquake History of the United States, NOAA, Publication 41-1, 1973.

McGuire, Robin K., Insights from the Chinese Catalog of Stationary Models Used for Seismic Hazard Assessment, USGS, Open File Report 77-715.

THE NEEDS OF THE NUCLEAR REGULATORY COMMISSION IN THE FIELD OF STRONG MOTION SEISMOLOGY

LEON REITER
U.S. Nuclear Regulatory Commission

The Nuclear Regulatory Commission (NRC) looks to the seismological and engineering community to help develop methods that provide reliable estimates of earthquake induced ground motion at different levels of risk for various sites throughout the country. These estimates should be in a form permitting effective use by geotechnical and structural engineers in the evaluation of sites and the design of structures for nuclear related facilities. Our needs generally parallel other engineering needs except that most nuclear facilities must be designed to be safe at very low levels of acceptable risk. Much recent research in strong motion seismology has been related directly or indirectly to nuclear power plant design so that our needs and problems have had an impact upon the trends within the science as a whole.

The problems we see today and the questions that we believe need answering can be divided into areas related to the earthquake source, seismic wave type and propagation, site effects, and engineering input.

EARTHQUAKE SOURCE

The most difficult problem we face today is estimating strong motion in the vicinity of the earthquake source, *i.e.*, the near-field. No nuclear power plant is intentionally placed near a known earthquake source or "capable" fault but subsequent investigations have revealed new faults and resulted in reassessment of some old faults. The Humboldt Bay, Diablo Canyon, San Onofre, and Vallecitos sites in California are the prime examples. In order to determine whether facilities at these sites are sufficiently safe as designed, need to be upgraded or need to be abandoned, requires an assessment of motion near earthquake sources where we have few measurements most of which are from small earthquakes. One approach has been to extrapolate inward from records taken at longer epicentral distances. How valid can this approach be when the particular physical and geometric configuration of the source, which apparently is dominant in controlling the near-field motion, is of secondary importance in the far-field. Are the more elegant theoretical models and numerical procedures for calculating the motion from these models in a stage where their results can be considered reliable?

Other aspects of the earthquake source problem relate to the eastern U.S. It has been postulated that intraplate earthquakes have higher stress drops than interplate earthquakes. If so can we expect and should we design for the increased amplitudes at the high frequencies believed to be associated with increased stress drops? While earthquakes in the East cannot be associated with surface faulting and the larger events appear to be occurring at hypo-

central depths of at least 10 kilometers, there are several occurrences of small near surface events that have resulted in very small felt areas of relatively high intensity. The magnitude 3.8, Intensity VII, event of August 14, 1965 in Cairo, Illinois is one such example. It is believed to have had a focal depth of approximately 1 km. These events have not been associated with structure. What magnitude may these events reach and what characterizes their ground motion?

WAVE TYPE AND PROPAGATION

Most present techniques such as those used to estimate soil response utilize models of ground motion which assume a predominance of vertically propagating, horizontally polarized shear waves. Studies of records such as those from the San Fernando earthquake show the importance of other types of waves, particularly surface waves. We must obtain better quantitative estimates of the different wave types involved in strong ground motion and the impact these will have upon structural design. To what extent does the existence of horizontally propagating waves result in the reduced effectiveness of an earthquake upon structures with large foundations? To what extent does the existence of these waves also result in rocking or torsional motions not previously considered?

A regional propagation difference is apparent between the eastern and western U.S. The much larger felt areas for similar sized earthquakes in the East necessitates consideration of the effect of distant (greater than 100 km) large events such as New Madrid. In what ways is damaging ground motion from these earthquakes different than that from sources less than 100 km away? Is increasing the long period part of the design response spectrum enough to account for the lower attenuation? If so, how much?

SITE DEPENDENCE

The most frequent problem we face is that of how to incorporate differences in site geology into estimates of free-field ground motions. Several investigators have classified sites in three or four broad categories and have shown differences in ground motion parameters such as peak acceleration and spectral shape associated with each category. The variation within each category however is rather large and it is not clear how significant the differences are. Investigations NRC has funded indicate that the surficial classification of accelerometer site conditions often is not confirmed by borings made in field investigations. All the comparative studies show relatively higher acceleration at rock for periods less than 0.5 sec. Since most safety related structures at nuclear power plants have periods equal to or less than 0.5 sec., does this mean it is less safe to build on rock than on soft sites? Observations of earthquake damage do not support this conclusion. Given the existing data base and state of our knowledge with respect to strong motion recording sites, how detailed a categorization is possible?

Along with differences in site properties the effects of depth upon ground motion are also of great importance. Present techniques of deconvolution need to be more uniformly

specified as to what ground motion is used and where the input is assumed. Are the present computational techniques adequate in providing estimates within a wide enough period range? Some individuals utilizing these techniques complain of irrational results which they attribute to the computational techniques. What are the limiting conditions to which deconvolution may be presently applied? Ground motion at depth is not only a problem with respect to foundations several tens of feet below the surface but is also of critical importance in the design of waste repositories at depths of hundreds or even thousands of feet.

ENGINEERING INPUT

Most present methods utilize standard response spectral shapes whose absolute level is determined by peak acceleration. The relatively high peak accelerations associated with some damaging earthquakes raises serious questions as to the validity of this approximation. Should we use other peak parameters such as velocity and displacement? Should we as some of us have suggested use a lower "effective" acceleration? If so how may this parameter be reliably estimated? Should we abandon reference values completely and go directly to each spectral ordinate given source and site characteristics? All the above questions assume that the response spectrum and related time history are seismological inputs that adequately describe ground motion for engineering purposes. Long durations however are not adequately reflected in the response spectra required by the NRC and are believed to be a critical factor in determining damage from large earthquakes. How, and to what extent, should duration of strong motion be incorporated into seismological input? Does it require a change in instrumentation so as to make a more faithful recovery of ground displacement? What is the duration to be considered in liquefaction studies?

Finally, any designed structures including those related to nuclear facilities entail the acceptance of some risk. Very often the most minimal of risks have to be weighed against other societal factors. Estimating these risks is a difficult and complex problem. The ability to place expected earthquake ground motion into a quantitative probabilistic framework would be an important contribution to arriving at both reasonable and reliable estimates of this risk.

SOME THOUGHTS ON THE DEFINITION OF THE INPUT EARTHQUAKE FOR THE SEISMIC ANALYSIS OF STRUCTURES

Jose M. Roesset
Massachusetts Institute of Technology

It has become customary in the seismic analysis of special structures, such as nuclear power plants, to define the input earthquake by a maximum ground acceleration (resulting from a seismic risk study with varying degrees of sophistication) and a family of smoothed universal response spectra. These spectra represent an envelope of the results for a collection of real earthquakes with different characteristics. One or more artificial earthquakes are then generated so as to match (more or less closely) the specified spectra, sealed to the desired peak ground acceleration. The motions are assumed to occur at the free-surface of the soil in the free-field (without disturbance by the structure).

This procedure is based on a series of simplifications which may be justified for an approximate design, but which appear inconsistent with the degree of refinement sought in the other phases of the analysis. The inconsistencies become more striking and may lead to unrealistic results when more complex methodologies, such as the use of probabilistic formulations or nonlinear dynamic analyses, are implemented. Efforts to improve this situation have not been, however, very successful in the past.

It would appear that more logical alternatives would be possible if we had the ability to construct realistic earthquake motions as a function of source mechanism, magnitude, epicentral distance, and overall geological and local soil conditions. One could then, in the seismic risk analysis, consider separately the various possible sources and derive for each one a probable motion, instead of lumping them together under the assumption of similar characteristics.

The specification of the design earthquake at the free-surface of the soil within the present procedure is reasonable when the soil can be classified as firm ground or with similar general characteristics as the sites at which the various records used to construct the envelope spectra were obtained. The use of these spectra for rock or for a very soft soil deposit would be, however, unrealistic.

Given the motion at the surface, it is normally necessary to make some assumptions as to the kind of waves that constitute the earthquake. For an embedded foundation, if the substructure method or three-step approach is used, it is first necessary to determine compatible motions (including rotations) at the foundation level, considering a massless foundation (this is the so-called kinematic interaction or wave scattering problem). But even if the foundation is at the surface and the input motion is applied directly at the base (including the soil compliances to account for soil structure interaction effects), one is in fact assuming implicitly that the horizontal motions are due to shear waves propagating vertically and the vertical motions are caused by vertically polarized P waves. When using the direct

SIMULATIONS OF EARTHQUAKE GROUND MOTIONS

Ralph A. Wiggins, Gerald A. Frazier,
Joel Sweet, and Randy J. Apsel

Delta Associates

A study has been undertaken to find a simple computer model that will simulate strong motion records near strike-slip earthquakes. The ultimate application for these simulations is for engineering design of structures. Hence, the study has been focused primarily on modeling response spectra at frequencies from 1. to 20. hz. The computer model has been tested by predicting response spectra for the 1940 Imperial Valley, 1966 Parkfield, and 1976 Brawley earthquakes.

The computer model that has been developed for simulating earthquakes is partitioned into three basic steps as described below.

FRACTURE SIMULATION

A three dimensional finite element code (SWIS) was used in conjunction with analytical solutions and laboratory experiments to provide information on how fault slip occurs during an earthquake (*Archuleta and Frazier*, 1978). Experiments performed on compressed rock specimens indicate that shear fracture occurs when the shear stress exceeds some limiting value in the neighborhood of one kbar. (The actual failure strength depends on rock composition, loading rate, the presence of cracks, confining pressure, and interspersed fluid.) The fracture strength of rocks can then be related to the maximum velocity of particles on the fault surface near the crack tip.

The physics of spontaneous shear fracture is contained in our characterization of fault slip. The following parameters are pertinent:

(a) Rupture Velocity: The rupture initiates at a point on the fault surface and spreads at a velocity which is taken as a fraction of the local shear wave velocity. Sensitivity studies have been performed with rupture velocity varying from 50% to 90% of the shear wave velocity, the upper limit being set at the Rayleigh wave velocity according to fracture mechanics.

(b) Dynamic Stress Drop: Large particle accelerations occur at points on the fault where new crack surface is being produced due to concentrations in stress. Immediately following the production of new crack surface, the shear stress drops to a lower value almost instantaneously. This effect is characterized in the slip function by a peak in the slip velocity at rupture initiation. This rapid slip, which can be related to dynamic stress drop using simplified mechanics, occurs for a brief interval of time while the crack extends a few tens of meters.

(c) Static Stress Drop: The static stress drop is a measure of the average difference in shear stress before and after an earthquake. The average final offset on the fault is linearly related to the static stress drop when the rupture area is held constant. After the initial peak, the slip velocity drops to a uniform value consistent with the static stress drop and rise time.

(d) Rise Time: Rise time is a measure of the duration of fault slip at a single point. SWIS calculations indicate that the rise time is controlled by the time it takes for information from non sliding portions on the fault surface to propagate to points where sliding is occurring. On the average, the rise time appears to be the time it takes for the shear wave velocity to traverse the fault width.

(e) Spatial Variations: In an actual earthquake, slip characteristics inevitably vary in some complex manner over the fault surface. In an effort to minimize the number of earthquake parameters the same slip function is used for all points on the rupture surface.

WAVE PROPAGATION

An analytical code (PROSE) has been developed to propagate seismic waves in horizontally layered, viscoelastic earth. The method accurately synthesizes the multiplicity of waves that arise in a horizontally layered medium over the frequency range from 0.1 to 20. Hz. Green's functions are obtained using the appropriate geologic layering for wave contributions that result from rapid slip over small fault segments which are distributed over the surface of impending rupture. Several hundred of these Green's functions are obtained for a single earthquake to insure accurate simulation of the seismic energy that radiates from all portions of the rupture surface.

The earth's crustal structure is characterized by horizontal, viscoelastic layers to a depth in excess of 20 km. Each layer is defined by the parameters: layer thickness, density, shear wave velocity, compressional wave velocity, and quality factor (Q). The quality factor for each layer is empirically related to the shear-wave velocity using both seismic evidence and laboratory data for guidelines. For cases in which conflicting evidence occurs, we have chosen to rely on that evidence with the largest quality factor, *i.e.*, we use the smallest material attenuation that is consistent with the available data.

GROUND MOTION

The fault slip, based on calculations by SWIS, is combined with the wave propagation produced by PROSE to produce synthetic earthquake motions using a convolution code (FALTUNG). The prescription of fault slip is convolved both in time and space over the rupture surface, with the elementary solutions from PROSE to produce synthetic ground motion at selected

points on the earth's surface over the frequency range from 0.1 to 20. Hz.

VALIDATION STUDIES

The range of validity of the computer model has been tested by simulating three past earthquakes -- Brawley (1976), Imperial Valley (1940), and Parkfield (1966). For all three earthquakes best fits are obtained for a rupture velocity of 90% of the shear wave velocity, a dynamic stress drop of 0.5 kbars, and a rise time set to the travel-time for shear waves to traverse the smallest fault.

Brawley -- Ground motions are modeled at an epicentral distance of 33 km using a 1.8 km-square rupture surface at a hypocentral depth of 7 km. A sufficiently good match is obtained between computed (see *Heaton and Helmberger*, 1977) and recorded ground motion to validate both the computer model and the geologic model for Imperial Valley. Sensitivity studies indicate that an adequate match with recorded signals depends critically on the size and depth of the rupture.

Imperial Valley -- Ground motions are computed at the El Centro recording station using a bilateral rupture which initiates 12.3 km to the southeast of the recording station. This rupture extends over a length of 48 km and a width of 12 km. Although an adequate fit to the response spectra is obtained by a linear bilateral rupture, the fit to the coda is improved by use of a rupture propagating along the crooked path of mapped surface break.

Parkfield -- Comparisons of the observed and computed response spectra show excellent agreement for the horizontal components of Stations 5, 8, and 12, using a 32 km long rupture with a width of 9 km. The computed vertical components are uniformly high in the mid-frequency range, but give good fits near the extreme frequencies of 0.1 and 20. Hz. Station 2 is so close to the fault that most of its response depends on local rupture properties, which are not resolved in this study. The geologic structure on the NE side of the fault is not the same as on the SW side; however, the fit to the Temblor Station is good.

As discussed above, some aspects of fault slip may be complicated beyond our ability to understand them in detail; however, rather uncomplicated characterizations can be used which explain earthquake data over a broad range of frequencies. Based on these studies, we conclude that our computer models can provide useful estimates of the frequency content of site specific ground motions for earthquake design purposes.

REFERENCES

Archuleta, Ralph J., and Gerald Frazier, 1978. Three-dimensional numerical simulations of dynamic faulting in a half-space: B.S.S.A., in press.

Heaton, Thomas H. and Donald V. Helmberger, 1977, Predictability of Strong Ground Motion in the Imperial Valley: Modeling the M4.9, November 4, 1976, Brawley Earthquake: in press.

DIRECTIONS OF FUTURE RESEARCH

As the Seminar-Workshop progressed, it became apparent that the major emphasis was on the Seminar portion, i.e., the mutual education of earthquake engineers and seismologists concerning the research work done by others. As a result, the final workshop session on the directions of future research tended to concentrate on a few points where opportunities for future research were clearly seen by all participants. Other directions, probably equally promising, were not discussed as much because many of the participants had not yet had time to reflect upon the things they had learned in the preceding discussions.

Although the nature of the Seminar-Workshop precluded a systematic examination of the directions of future research, some of the points of mutual interest that emerged in the discussion are summarized below:

1. Modeling of Strong Ground Motion. Recent developments in research have made Seismologists believe that reliable modeling of ground motion is possible for periods of one-second and longer, using deterministic models of source mechanisms and travel paths. Earthquake engineers on the other hand, have made considerable progress in empirical and statistical modeling of strong ground motion. The combination of these approaches seems promising and some interesting results are already starting to come forth.

2. Transmission of Strong Ground Motion. Earthquake engineers have developed simplified methods of analyses for assessing the earthquake response of soil profiles, buried pipelines, buildings with significant soil-structure interaction, etc., under the action of different type waves. For example, vertically polarized SH-motions are often assumed, and occasionally Rayleigh or Love waves. There is a need to incorporate more seismological information and insight into these processes so that more realistic partitioning of the energy into different wave types can be performed.

3. The Use of Aftershocks. The recent studies of the Oroville earthquake sequence have shown that much significant information of interest to both engineers and seismologists can be gained from measuring strong motion aftershocks. Because the location of strong aftershocks is known once the main shock occurs, and because there is a general assurance of obtaining many strong-motion accelerograms in a period of weeks or months, the increased study of aftershocks appears quite promising.

4. The Characterizations of Earthquake Motion for Design. Earthquake engineers and Seismologists are heavily involved in the determination of the earthquake-resistant design criteria for major projects, such as large dams and nuclear powerplants, LNG facilities, etc. The improved characterization of the earthquakes and resulting ground motions that are critical to the design of the facilities is an area of promising research with potentially large benefits.